

Lifelong calorie restriction affects indicators of colonic health in aging C57Bl/6J mice

Kok, D. E. G., Rusli, F., van der Lugt, B., Lute, C., Laghi, L., Salvioli, S., ... Steegenga, W. T.

This is a "Post-Print" accepted manuscript, which has been published in "Journal of Nutritional Biochemistry"

This version is distributed under a non-commercial no derivatives Creative Commons  (CC-BY-NC-ND) user license, which permits use, distribution, and reproduction in any medium, provided the original work is properly cited and not used for commercial purposes. Further, the restriction applies that if you remix, transform, or build upon the material, you may not distribute the modified material.

Please cite this publication as follows:

Kok, D. E. G., Rusli, F., van der Lugt, B., Lute, C., Laghi, L., Salvioli, S., ... Steegenga, W. T. (2018). Lifelong calorie restriction affects indicators of colonic health in aging C57Bl/6J mice. Journal of Nutritional Biochemistry, 56, 152-164. DOI: 10.1016/j.jnutbio.2018.01.001

You can download the published version at:

https://doi.org/10.1016/j.jnutbio.2018.01.001

Manuscript: Lifelong calorie restriction affects indicators of colonic health in aging C57Bl/6J mice

Authors: Dieuwertje EG Kok[a*], Fenni Rusli[a], Benthe van der Lugt[a], Carolien Lute[a], Luca Laghi[b], Stefano Salvioli[c], Gianfranco Picone[b], Claudio Franceschi[c], Hauke Smidt[d], Jacques Vervoort[e], Ellen Kampman[a], Michael Müller[f] and Wilma T Steegenga[a]

[a] Division of Human Nutrition, Wageningen University & Research, 6708 WE, Wageningen, The Netherlands
[b] Centre of Foodomics, Department of Agro-Food Science and Technology, University of Bologna, 47521, Cesena (FC), Italy
[c] Department of Experimental, Diagnostic and Speciality Medicine, University of Bologna, 40126, Bologna, Italy
[d] Laboratory of Microbiology, Wageningen University & Research, 6708 WE, Wageningen, The Netherlands
[e] Laboratory of Biochemistry, Wageningen University & Research, 6708 WE, Wageningen, The Netherlands
[f] Nutrigenomics and Systems Nutrition Group, Norwich Medical School, University of East Anglia, NR4 7UQ, Norwich, UK

Corresponding author:
Dieuwertje E Kok, PhD
Division of Human Nutrition, Wageningen University & Research
PO Box 17, 6700 AA Wageningen, The Netherlands
Telephone: + 31 317 485 901, Email: dieuwertje.kok@wur.nl

ABSTRACT

Diminished colonic health is associated with various age-related pathologies. Calorie restriction (CR) is an effective strategy to increase healthy lifespan, although underlying mechanisms are not fully elucidated. Here, we report the effects of lifelong CR on indicators of colonic health in aging C57Bl/6J mice. Compared to an *ad libitum* control and moderate-fat diet, 30% energy reduction was associated with attenuated immune- and inflammation-related gene expression in the colon. Furthermore, expression of genes involved in lipid metabolism was higher upon CR, which may point towards efficient regulation of energy metabolism. The relative abundance of bacteria considered beneficial to colonic health, such as *Bifidobacterium* and *Lactobacillus*, increased in the mice exposed to CR for 28 months as compared to the other diet groups. We found lower plasma levels of interleukin 6 and lower levels of various metabolites, among which bile acids, in the colonic luminal content of CR-exposed mice as compared to the other diet groups. Switching from CR to an *ad libitum* moderate-fat diet at old age (24 months) revealed remarkable phenotypic plasticity in terms of gene expression, microbiota composition and metabolite levels, although expression of a subset of genes remained CR-associated. This study demonstrated in a comprehensive way that CR affects indicators of colonic health in aging mice. Our findings provide unique leads for further studies that need to address optimal and feasible strategies for prolonged energy deprivation, which may contribute to healthy aging.

Keywords: aging; calorie restriction; colonic health; gene expression; gut microbiota; metabolites

1. INTRODUCTION

Aging is characterized by a time-dependent accumulation of cellular and molecular damage, which in turn results in various age-related morbidities [1-3]. To date, the most effective strategy to improve both health and lifespan in various model organisms is calorie restriction (CR), which refers to a reduced energy intake (usually 30-40% restriction) without malnutrition [4, 5]. Also for humans, emerging evidence suggests that CR is associated with physiological, metabolic and molecular adaptations that may, at least partly, contribute to improved metabolic and molecular health [6].

The mechanisms underlying the effects of CR are, despite extensive research, only partially understood. A complex interplay between metabolic adaptations, immune responses and other molecular processes are thought to be responsible for the health-promoting and life-extending effects of CR [7, 8]. Attenuation of chronic low-grade and age-related inflammation, also called inflammaging [9], is considered a plausible mechanism via which CR prevents or delays common pathologies such as cancer, cardiometabolic diseases and cognitive decline [10-13].

Emerging evidence shows that a disturbed balance between beneficial and harmful bacteria is one of the driving forces behind inflammaging [14, 15]. From this perspective, the colon plays a pivotal role in maintenance of health during aging as the intestinal epithelial barrier function and permeability determine interaction with the intestinal microbiota and the external environment [16, 17]. We have previously shown that aging is accompanied by changes in expression of genes related to inflammation and enhanced immune responses in the colon of aging mice [18]. Also age-related changes in microbiota composition and bacterial metabolites, including short chain fatty acids, have been described in aging populations of rodents and humans [15, 19-21].

Interestingly, it has been shown that CR is able to alter the intestinal microbiota composition in aging mice [22]. The potential of CR to suppress detrimental processes in the colon, such as carcinogenesis [23, 24], further emphasizes that CR is a plausible and powerful candidate that may support maintenance of colonic health during aging. However, detailed insight into persistence of CR-induced effects upon challenging conditions is scarce [25]. It has been demonstrated that favourable metabolic effects are persistent after discontinuation of prolonged CR [26, 27]. To what extent this ‘metabolic memory’ also applies to the colon, and whether CR-induced effects on markers of colonic health are persistent, is not known.

In this study, we provided a comprehensive overview of the molecular, microbial and metabolic effects of lifelong CR, referring to 30% energy reduction without malnutrition, in the colon. The effects of

CR were contrasted against a control diet (C) and a Western-style moderate-fat (MF) diet. Microbiota composition, whole-genome gene expression profiles, levels of metabolites and circulating cytokines were determined in male C57BL/6J mice at young (6 months) and old age (28 months). At 24 months of age, a subgroup of mice was transferred from CR to an *ad libitum* MF diet (CR>MF). This diet switch provided the unique opportunity to study phenotypic plasticity in CR-exposed mice.

2. MATERIALS AND METHODS

2.1 Animals and diets

The design of the study and experimental procedures have been described in detail previously [28, 29]. Briefly, male C57BL/6J mice were individually housed and randomized to different dietary regimens at the age of 9 weeks. For the current analyses, we considered mice that were lifelong fed a semi-synthetic control diet consisting of 10E% of fat (C), a CR diet without malnutrition (30% energy reduction compared to the C diet) or a MF diet consisting of 25E% of fat (**Supplementary Table A.1**). All diets, except the CR diet, were fed *ad libitum*. Mice sacrificed at 6 or 28 months of age were considered in order to differentiate between effects at young and old age. To study the molecular flexibility and dynamics after receiving a strict CR diet for prolonged time, a diet switch was included in this study. A subgroup of mice on CR (n=16) was switched to the MF diet at the age of 24 months until sacrifice at 28 months.

Upon sacrifice at 6 or 28 months of age, colon and plasma samples were collected for 11-18 mice per intervention group. The mice were fasted for 4 hours prior to sacrifice after which they received an intragastric gavage of either solvent (mock: 0.5% carboxymethyl cellulose) or Wy-14643 dispersed in solvent (160 mg Wy-14643/kg body weight) and were then fasted again for another 6 hours. The purpose of the treatment with Wy-14643, which is a PPARα agonist, was to examine PPARα adaptive capacity in the liver, which has been covered in a separate publication [30]. Since Wy-14643 can cause fast and pronounced effects on gene expression in various organs [31, 32], only mock-treated mice were considered for the gene expression analyses. For the analyses of the microbiota composition and plasma Il6 levels Wy-treated mice were additionally included to increase the statistical power. Results on food intake, body weight development, survival characteristics and liver transcriptome data of the mice have been published elsewhere [33].

At sacrifice, blood samples were collected by cardiac puncture. The colon was opened longitudinally and colonic luminal contents were obtained by flushing faecal pellets with phosphate-buffered saline (PBS) and immediately stored at -80°C. The colonic luminal content samples were used for metabolite and

microbiota profiling. Scrapings of the mucosa and submucosa from the distal and proximal segments of the colon were collected, snap frozen in liquid nitrogen and stored at -80°C for whole-genome gene expression profiling. At the age of 28 months, urinary samples were collected on consecutive days until a total of 1 mL was obtained. Individual mice were held above a clean and empty petri dish and the urine was transferred to an Eppendorf tube which was stored at -80°C. The design of the study and the experiments described were approved by the Local Committee for Care and Use of Laboratory Animals at Wageningen University (drs-2010151b).

2.2 Circulating levels of cytokines

Plasma levels of interleukin 6 (Il6) were determined at 6 and 28 months of age (n=8-17 mice per diet group) using the customized Mouse Adipokine Magnetic Bead Panel MILLIPLEX® MAP assay (kit MADKMAG-71K, Merck Millipore, Darmstadt, Germany) according to the manufacturer's protocol. Data were log (base2) transformed for visualisation and statistical analyses.

2.3 RNA isolation and gene expression analyses

To determine the transcriptional effects of the different dietary regimens, whole-genome gene expression profiles were studied in the colonic scrapings of mice at 6 and 28 months of age. Colonic samples from 44 mice, ranging from 5-7 mice per group, were analysed. Total RNA was isolated from the scrapings using TRIzol Reagent according to the manufacturer's instructions (Invitrogen, Breda, The Netherlands). Isolated RNA was purified using RNeasy Micro columns (Qiagen, Venlo, The Netherlands) and total RNA yield (Nanodrop ND-1000, Nanodrop Products, Maarssen, The Netherlands) and RNA integrity (Agilent 2100 Bioanalyzer, Agilent Technologies, Amsterdam, The Netherlands) were assessed for all samples.

Purified RNA (100 ng per sample) was converted to cDNA and labelled using an Ambion WT expression kit (Life Technologies, Bleiswijk, The Netherlands). Samples were hybridized to the Affymetrix GeneChip Mouse Gene 1.1 ST array according to the standard Affymetrix protocols (Affymetrix, Santa Clara, CA, USA). Two samples did not pass the quality control and were excluded, resulting in a total of 42 samples with microarray data available. The arrays were normalized using the Robust Multichip Average (RMA) approach [34]. Probe sets were defined according to Dai et al. [35] using the chip description file (CDF) version 19.0.0 based on the Entrez Gene database. Genes that had a RMA expression value >20 in at least 5 arrays were considered expressed. Only those genes with an interquartile range (IQR) >0.1 for all samples together were included in the analyses, resulting in a total of 16,071 genes. Differences in gene expression between the diet groups were analysed using the Intensity Based Moderated T statistics (IBMT) [36] with p-values <0.01 as threshold. Microarray data are available from the Gene Expression Omnibus (GEO) repository with number GSE100701.

2.4 Determination of the microbiota composition based on 16S rRNA gene profiling

Microbiota composition was determined in the colonic luminal content of 8-10 mice per diet group at the age of 6 and 28 months, resulting in a total of 68 samples. Genomic DNA was extracted from the colonic luminal content using the ZR Fecal DNA MicroPrep kit (ZYMO Research, Irvine, CA, USA) according to the instructions of the manufacturer. Subsequently, the V3-V4 region of the 16S ribosomal RNA (rRNA) gene was amplified using a 2-step PCR. First, 10-25 ng of DNA was amplified using the 341F (5'-CCTACGGGNGGCWGCAG-3') and 785R (5'-GACTACHVGGGTATCTAATCC-3') primers appended with Illumina adaptor sequences. Amplicons were purified using the ZR-96 DNA Clean and Concentrator-5 Kit (ZYMO Research, Irvine, CA, USA). To quantify DNA content of the resulting amplicon, the Qubit® Fluorometric Quantitation device (ThermoFisher Scientific, Waltham, MA, USA) was used. Besides, the amplicons were run on a 2%-agarose gel to confirm amplicon size and amount. Purified PCR products were used for the second PCR in combination with sample-specific barcoded primers (Nextera XT index kit, Illumina, San Diego, CA, USA). Purified PCR products with an amplicon length of 550 base pairs (bp) (including adaptors) were submitted for sequencing in the paired-end (2x) modus (300 bp) on the MiSeq platform (Illumina, San Diego, CA, USA) at the BaseClear service laboratory (BaseClear BV, Leiden, The Netherlands). FASTQ files were generated and de-multiplexed based on sample-specific barcodes using the Casava pipeline (version 1.8.3, Illumina, San Diego, CA, USA). Sequence reads of low quality (only "passing filter" reads were selected) or containing the adapters or PhiX control signals were removed and the FASTQC pipeline (version 0.10.0, http://www.bioinformatics.babraham.ac.uk/projects/fastqc/) was applied for the initial quality control. One sample was excluded (old mouse on MF diet) because the coverage was below the threshold (50% of the median number of reads).

Further pre-processing of the sequencing data, including merging of the paired reads and fixed length trimming of the reads (cut-off is mean length of the merged reads minus one standard deviation) was performed using the CLC Microbial Genomics Module (version 1.2.1, CLC Bio, Qiagen, Aarhus, Denmark) in the CLC Genomics Workbench (version 8.5.1, CLC Bio, Qiagen, Aarhus, Denmark). Based on a total of 763,543 reads, 1017 OTU (operational taxonomic unit) groups were identified after alignment against the Silva database [37] at 97% similarity. For 31 of these OTUs (225 reads in total), taxonomic annotation could not be retrieved (N/A). Differences in relative abundances for the diet or age groups were determined using a Kruskal Wallis test with Bonferroni correction for multiple comparisons (adjusted $p<0.05$). Dunn's post hoc comparisons (adjusted p-value <0.05) were performed to further explore the contrasts and identify genera that differed between the diet groups at young or old age.

The CLC Microbial Genomics Module was also used to determine the alpha and beta diversities. For these analyses, all OTU's with a combined number of ≥ 10 reads were considered. The Shannon entropy

was used as a measure for alpha-diversity (richness and evenness). The beta diversity, showing differentiation of the taxa among the different samples, was determined using Bray-Curtis distances. Individual samples were visualized in corresponding principal coordinate analyses (PCoA) plots for the first two principal coordinates. Canoco 5 (Windows release 5.0.4) was used for constrained multivariate data analyses [38]. A redundancy analysis (RDA) was performed with reads (compositional data) as the response variable and the diet groups as the explanatory variable. For this RDA, the 242 OTUs with a relative abundance of ≥0.1% in at least one sample were considered. Numbers of reads were centered and standardized using the Hellinger approach to assign low weights to rare species [39]. The 16S rRNA gene data described in this study have been deposited in the sequence read archive (SRA) at the NCBI with accession number SRP118464.

2.5 Levels of short chain fatty acids and other metabolites in the colonic luminal content

Levels of short-chain fatty acids and other metabolites were determined in the colonic luminal content of 6-8 mice per group using proton nuclear magnetic resonance (^{1}H-NMR) as described previously [40]. Briefly, minimal two pellets of colonic luminal content were weighed, diluted (~1:5) and lysed with a TissueLyser (Qiagen, Hilden, Germany) in phosphoric buffer (in 100 mM, pH 8.0). After centrifugation, 200 µL of the supernatant was transferred to a 3 mm NMR tube (Bruker match system) and measured as described previously [40]. From the aligned spectra, integrals for metabolites of interest (SCFAs and succinate) as well as other metabolites that differed between the intervention groups were selected and quantified. The untargeted approach resulted in the identification of several bile acids that differed between the groups (chemical shifts between 0.7-0.8 ppm). A total of 6 reference compounds (sodium cholate hydrate, sodium glycodeoxycholate, sodium glycocholate hydrate, sodium deoxycholate, sodium taurocholate hydrate, sodium taurodeoxycholate hydrate) were carefully titrated to the samples to provisionally annotate the identified metabolites. Obtained integrals were adjusted for the dilution factor. Concentrations of metabolites were calculated based on the number of hydrogens for each metabolite selected.

2.6 Urinary metabolites

Urinary samples (1 mL) were collected for 7-9 mice per group at the age of 28 months. The urinary samples were sent to the University of Bologna (Bologna, Italy) for metabolomics analyses using ^{1}H-NMR as described previously [41]. Briefly, spectra were recorded at 298K with an AVANCE III spectrometer (Bruker, Milan, Italy) at a frequency of 600.13 MHz. The obtained NMR spectra were adjusted for baseline values through the simultaneous peak detection and baseline correction algorithm (SPDBC) implemented in the 'baseline' R package [42, 43]. An in-house modified version of the correlation optimized shifting (i-

Coshift) was applied to adjust for errors in chemical shift misalignments in localized regions of the spectrum [44] and spectra were normalized by means of the probabilistic quotient normalization method in order to adjust for the water content in the urine [45]. Spectra were subsequently converted to metabolic profiles and quantified by comparing their chemical shift and multiplicity with the Human Metabolome Database [46] and Chenomx software data bank (version 7.7, Chenomx Inc., Edmonton, Canada). In total, 58 unique signals were identified, of which 50 were assigned to specific metabolites. Quantification is based on the conversion of selected integrals (free from interference) to concentrations (values expressed as nM) after comparison to the internal standard (tri-methyl-silyl-propionate).

Supervised partial least square discriminant analyses (PLS-DA) were performed on the concentrations of the metabolites in order to visualize the trends of sample clustering (score plot) and to explore the discriminating metabolites specific for the diet groups at 28 months (loading plot). The R package 'DiscriMiner' was used for PLS-DA with the Leave-One-Out (LOO) approach for cross validation. To confirm the separation of samples, also principal component analyses (PCA) were performed in order to visualize unsupervised clustering of samples. At the level of the individual metabolites, non-parametric Kruskal Wallis tests and Dunn's post hoc tests were performed in order to compare concentrations of selected urinary metabolites between the diet groups.

2.7 Multivariate analyses

In order to integrate the various comprehensive molecular datasets, multivariate analyses were performed using the mixOmics package [47] in R 3.1.2. Correlations between microbiota composition in the colonic luminal content and colonic gene expression profiles in the colonic scrapings were assessed using a partial least square (PLS) analysis in the 'canonical' mode to assess the bi-directional relationships [47]. For 40 individual mice, data on microbiota composition and gene expression were available. Microbiota composition was considered at the genus level. Only genera with at least 10 combined reads for all the samples were considered resulting in 56 genera included in the analyses. Prior to analyses, the MiSeq sequencing reads for the different genera were transformed and zeros were imputed based on the centered log ratio (clr) using the aldex2 package with 1024 monte Carlo permutations [48]. Gene expression data were considered as log2 transformed RMA intensities. The 1000 genes with most variable expression (highest interquartile ranges for log2 RMA values) at the age of 28 months were analysed together with the 56 genera. Hierarchical clustering based on the Euclidian distance was applied for the identification of the six main clusters for both the genes and the genera. The gene ontology (GO) of the biological processes was further explored for the identified gene clusters with the Enrichr enrichment analysis tool [49, 50].

Relevance networks for the genes and genera with most pronounced pairwise correlations ($r \leq -0.75$ or $r \geq 0.75$) were visualized using Cytoscape [51].

2.8 Statistical considerations

IBM SPSS Statistics 22 for Windows (Armonk, NY, USA) and the R statistical environment (R 3.1.2) were used for the statistical analyses unless otherwise described. Differences between the diet groups were determined with Kruskal Wallis tests for non-parametric data. Dunn's post hoc comparisons were performed to further explore the contrasts and identify differences between the diet groups at young or old age. For data following a normal distribution, a one-way analysis of variance (ANOVA) followed by a post hoc Tukey's test was used to compared the different diet groups at young or old age. Whenever appropriate, statistical analyses were adjusted for multiple testing using the Bonferroni or Benjamini-Hochberg approach.

3. RESULTS

3.1 CR affects expression of genes implied in the immune response and inflammation

Gene expression profiles were determined in mucosal scrapings collected at 6 and 28 months of age to identify biological pathways regulated by CR. At 6 months, mice on CR showed differential expression for 825 genes compared to the C diet and 897 genes compared to the MF diet (**Figure 1A**). At 28 months, 657 and 449 genes were differentially expressed comparing CR versus the C and MF diet, respectively. Several genes involved in lipid metabolism were up-regulated in the mice exposed to CR as compared to MF (**Table 1**). Among these, potential PPAR target genes such as *Lpl*, *Scd1* and *Fads1* were identified in mice exposed to CR during aging. Genes most pronouncedly down-regulated upon CR included genes encoding for immunoglobulins and the B-cell antigen receptor complex (Cd79a and Cd79b), S100g / calbindin-D9k, and the antimicrobial factors Lyz1 and Ang4 (**Table 1**).

Ingenuity pathway analysis (IPA) revealed that affected canonical pathways for the comparison between CR and MF were predominantly related to immune responses, and specifically involvement of B-lymphocytes and T-lymphocytes (**Figure 1B**). Lipopolysaccharide (LPS) as well as various chemokines and cytokines, such as interleukin 2, 6, 15 and 21, tumor necrosis factor (Tnf), interferon gamma (Infg) and the Spi-1 proto-oncogene (Spi1), were identified as potential upstream regulators responsible for the observed differences in gene expression (**Supplementary Table A.2**). A subset of genes was differentially expressed between CR and the MF diet both at young and old age (overlap n=135 genes, **Figure 1C**).

Pathway and regulatory analyses for both ages consistently showed attenuation of expression related to immune responses and inflammation in the colon of mice exposed to CR.

To determine whether CR also affected systemic markers of inflammation, circulating levels of interleukin 6 (Il6) were measured in plasma. Levels of Il6 were significantly lower in the mice exposed to CR as compared to the C ($p<0.05$) or CR>MF diet ($p<0.01$) at old age (**Figure 1D**).

3.2 Gene expression profiles largely adapt to the MF diet after a diet switch at old age

Principal component analyses (PCA) based on the 1000 most variable genes at old age showed that the diet switch (CR>MF) resulted in gene expression profiles that largely resembled profiles of mice on the MF diet (**Figure 1E).** To further investigate persistence or adaptation of expression profiles in the colonic scrapings, we identified genes that were specifically associated with either CR or MF in the diet switch group (**Figure 1F**). Based on 449 genes that were differently expressed between CR and MF, we recognized 27 genes that remained similar to the CR group ($p>0.01$ for CR versus CR>MF) (**Supplementary Table B.1**). Besides several immunoglobulin-related genes, mucin 20 (*Muc20*) was one of the most prominent CR-associated genes after the diet switch (**Figure 1G**).

Equally, 161 MF-associated genes were identified (**Supplementary Table B.1**). Stearoyl-CoA desaturase-1 (*Scd1*) was one of the most prominent adapted genes (**Figure 1H**). This key enzyme in fatty acid regulation was highly expressed in mice exposed to CR, but expression was strongly diminished after the diet switch. Besides *Scd1,* other genes involved in metabolic processes also adapted to the MF expression profile. **Supplementary Figure A.1** shows a network of genes and related molecules involved in lipid metabolism and energy production that shifted towards the MF profile.

In conclusion, gene expression profiles in the colon and circulating levels of Il6 suggest an attenuated immune response and anti-inflammatory profile in mice exposed to lifelong CR. Switching from CR to an *ad libitum* MF diet at old age resulted in physiological and molecular adaptation. Given the central role of LPS as predicted regulator for gene expression, plausible effects of the dietary regimens on intestinal microbiota composition were further investigated.

3.3 The CR diet determines microbiota profiles that are not persistent after a diet switch

Microbial profiling of the colonic luminal content based on Illumina MiSeq sequencing of PCR-amplified 16S rRNA gene fragments resulted in an average of 27,340 reads (standard deviation: 7,940) per sample. The Shannon entropy, indicating richness and evenness, did not statistically significantly differ between the groups (**Figure 2A**). Analyses at the phylum level revealed that Firmicutes were less abundant, whereas Actinobacteria and Verrucomicrobia were more abundant in young mice exposed to CR as compared to the

C and MF diet (**Figure 2B**). Likewise, Actinobacteria (<1%) as well as Verrucomicrobia (<1%) were hardly detected in old mice on the C or MF diet, whereas these phyla were more abundant (8% and 4%, respectively) in mice on lifelong CR. In old mice on the MF diet, relative abundance of the Tenericutes increased (2%) as compared to the other diet groups (<0.1%). Differences in microbial composition between samples estimated based on the Bray-Curtis dissimilarity showed that CR clearly separated from the C and MF diet (**Figure 2C**). Switching from CR to MF resulted in microbial profiles that largely resembled that of mice fed the C and MF diet.

More in-depth analyses of the microbiota composition in the colonic luminal content revealed that for 26 genera the relative abundance differed for the respective diet groups (Kruskal Wallis test, $p<0.05$ with Bonferroni correction, **Figure 2D**). At both 6 and 28 months, CR-exposure specifically resulted in higher relative abundance of *Bifidobacterium* and *Lactobacillus* genera as compared to the C or MF intervention group. A member of the *Peptostreptococcaceae* family, *Clostridium sensu stricto 1* and *Turicibacter* genera were less abundant or absent in the mice on CR. Some genera showed age-related changes in relative abundance, which was markedly attenuated by CR (**Figure 2E**). The relative abundance of *Akkermansia*, *Parasutterella*, *Bifidobacterium*, *Allobaculum* and an unclassified member of the *Coriobacteriaceae* family increased, whereas for *Desulfovibrio, Bilophila*, *Turicibacter*, and few others relative abundances decreased during aging upon CR-exposure as compared to the other diet groups. In line with the pronounced microbial signatures affiliated with the respective diet groups, body weight at sacrifice also showed modest to strong inverse correlations with relative abundance of several genera, including *Akkermansia, Bifidobacterium, Parasutterella* and others (**Figure 2F** and **Supplementary Table A.3**). Similar results were observed when epididymal white adipose tissue (in % of body weight) was considered in relation to relative abundance of these genera (**Supplementary Table A.3**).

Taken altogether, these data indicate that CR strongly influenced colonic microbiota composition and that lifelong exposure to CR protected against age-related shifts in microbiota composition. Switching from CR to an *ad libitum* MF diet resulted in microbial profiles that largely adapted to the MF diet (**Figure 3A**). Multivariate redundancy analyses (RDA) revealed that discriminating OTU signatures specific for CR include *Parasutterella*, *Lactobacillus* and *Bifidobacterium* genera. The diet switch was associated with a signature that resembled that of mice fed the C and MF diet at old age (including genera of *Blautia*, *Roseburia*, *Desulfovibrio* and others, **Figure 3B**). These findings indicate that the microbiota profiles in aging mice are dynamic and sensitive to dietary changes, even after lifelong adherence to a strict CR regimen.

3.4 Integration of microbiota composition data and gene expression profiles

To reveal whether microbiota composition in the colonic luminal content and gene expression in the colonic scrapings were correlated, transcriptomic and microbiota datasets were integrated based on data of individual mice. The 1000 most variable genes at old age showed pronounced correlations with microbiota composition at the genus level (**Figure 4A**). The two main identified gene clusters referred to biological processes implied in muscle system processes and inflammation (gene cluster 2, 181 genes) or B-cell activation (cluster 3, 152 genes) (**Table 2**). Gene cluster 2 and 3 were positively correlated with microbiota cluster D, which included *Clostridium sensu stricto 1*, *Turicibacter*, *Roseburia, Bilophila* and various members of the *Ruminococcaceae* and *Lachnospiraceae* families *(***Table 2***)*. An inverse correlation for genes in cluster 2 and 3 was found for *Lactobacillus*, *Bifidobacterium,* an unclassified *Coriobacteriaceae* and the *Parasutterella* genera in cluster F, whereas also *Parabacteroide*s and *Bacteroides* in cluster E were inversely associated with this gene cluster (**Figure 4A**).

Focussing on the most pronounced ($r<-0.75$ or $r>0.75$) correlations in a network analysis indicated that mainly the *Parabacteroides* genus was inversely correlated to genes involved in extracellular matrix organization, cellular migration, and immune-related genes (**Figure 4B**). Also *Parasutterella*, *Bifidobacterium* and an unclassified member of the *Coriobacteriaceae* family were inversely correlated to several immune-related genes, including genes involved in the innate immune response (*Cybb*, *Cxcl13*). *Roseburia*, *Turicibacter* and an unclassified member of the *Ruminococcaceae* family showed positive correlations for the same genes. Altogether, these results showed that microbiota composition and gene expression profiles in the colon were correlated.

3.5 Metabolic signatures show lower bile acid levels in the colon of mice on CR

To strengthen evidence for causal relationships between microbiota composition and gene expression, we determined whether metabolites in the colonic luminal content were affected by the dietary interventions. Specifically, levels of short-chain fatty acids (SCFAs) and succinate, as major microbial end-products, were determined by ^{1}H-NMR analyses. Levels of butyrate, acetate and propionate did not differ between dietary regimens within the specific age groups (**Figure 5A-C**) and substantial variation between individual mice was observed. Levels of succinate were higher in the colonic luminal content of old mice on CR as compared to the C diet ($p<0.05$) (**Figure 5D**).

Further exploration of the ^{1}H-NMR spectra showed that levels of several bile acids in the colonic luminal content showed pronounced variation for the different diet groups and ages. Four bile acids could be identified and annotated based on the ^{1}H-NMR spectra and reference compounds carefully titrated to the samples: 1) cholic acid (CA), 2) deoxycholic acid (DxCA) or taurodeoxycholic acid (TDxCA), 3)

chenodeoxycholic acid (ChDxCA), and 4) a ChDxCA derivate [52]. Levels of the primary bile acid CA did not differ between the diet groups, whereas levels of ChDxCA and the secondary bile acids (DxCA / TDxCA and a ChDxCA derivate) were lower in mice exposed to CR as compared to the other diet groups (**Figure 5E-H**). Levels of these bile acids were inversely correlated with relative abundance of *Lactobacillus* and *Bifidobacterium* and few other genera in the colonic luminal content (for the ChDxCA derivate: Spearman r=-0.824 for *Bifidobacterium*, r=-0.750 for *Lactobacillus* and r=-0.733 for *Parasutterella*) and positively correlated with relative abundance of for example *Turicibacter* (r=0.702) and an uncultured *Peptostreptococcaceae* (r=0.624) (**Figure 5I**).

Also urinary metabolites were determined in old mice. From ^{1}H-NMR spectra of the urine samples, 58 molecules were identified. Both supervised partial least square discriminant analyses (PLS-DA) and unsupervised (PCA) analyses clearly showed clustering of the mice per diet group (**Figure 6A, 6C, 6D**). Mice exposed to lifelong CR appeared to have different urinary metabolite profiles compared to C and MF diets. Metabolites related to the tricarboxylic acid cycle (TCA) cycle, such as succinate, fumarate, citrate, cis-aconitate and 2-oxoglutarate, were more abundant in mice on CR as compared to the C or MF group (**Figure 6B**, **6E**). Interestingly, also levels of other metabolites, such as 2-hydroxyisobutyrate which is a microbial metabolite and is associated with adiposity [53], differed between the intervention groups (**Figure 6F**).

4. DISCUSSION

The results of this study, unique for its integration of molecular, microbial and metabolic parameters, showed that lifelong CR induced pronounced effects in the colon of aging mice. Our findings strongly support the hypothesis that CR prevents or delays the aging-induced decline in colonic health by modulating the immune response and protection against chronic low-grade inflammation [54, 55]. Moreover, we speculate that the colonic gene expression profiles related to lipid metabolism and urinary TCA metabolites are pointing towards efficient regulation of energy metabolism in mice exposed to CR. Molecular, microbial and metabolic patterns showed adaptation after switching from CR to an *ad libitum* MF diet, although a small subset of genes remained CR-associated.

Several mechanisms have already been proposed to explain the health-promoting or life-extending effects of CR [7, 8]. Based on our gene expression data, CR-induced effects in the colon seemed to be dominated by alterations in immune- and metabolism-related processes. Our findings are consistent with various studies showing that CR affected markers of immune function or reduced expression of inflammatory genes in different tissues and model species [54, 56, 57]. The imbalance between pro- and

anti-inflammatory stimuli and subsequent manifestation of chronic, low-grade inflammation during aging are well-known for their involvement in age-related diseases [9]. The intestinal microbiota has been suggested as one of the contributors to chronic low-grade inflammation, possibly through LPS or other microbial products [58-60]. In our study, LPS was identified as one of the main upstream regulators predicted to be responsible for gene expression differences between CR and MF. Moreover, down-regulated expression of *Lyz1* and *Ang4*, two genes encoding for antimicrobial proteins, as well as lowered plasma levels of Il6 may imply that mice on CR were exposed to less pro-inflammatory stimuli. According to recent insights, the intestinal microbiota is considered a critical determinant of pro- as well as anti-inflammatory stimuli [60].

Progressive changes in microbiota composition during aging have been described in humans and mice [14, 20, 61]. Our study adds evidence that CR is able to diminish age-related shifts in the intestinal microbiota. Especially age-related declines in relative abundance of *Bifidobacterium*, *Akkermansia*, *Allobaculum*, *Parasutterella* and an unclassified member of the *Coriobacteriaceae* family were prevented in mice on CR. *Bifidobacterium* and *Parasutterella* were, besides *Parabacteroides*, also the most pronounced genera inversely associated with the expression of genes involved in the immune response and extracellular matrix organization. *Bifidobacterium* spp. have been previously recognized for their immune-modulatory and anti-inflammatory effects and are therefore considered beneficial for colonic health [62, 63]. We identified an unclassified genus of the *Coriobacteriaceae* family, which showed similar correlation patterns as the *Bifidobacterium* genus. The functional relevance of these findings remains speculative, however, relative abundance of the *Coriobacteriaceae* was previously reported to be lower in children with inflammatory bowel diseases as compared to healthy controls [64]. Besides, the *Coriobacteriaceae* family was implied in energy and lipid metabolism in mice [65]. These findings may provide leads for further research focussing on the potential beneficial effects of *Coriobacteriaceae* with regards to colonic health.

We demonstrated that several genera that were positively correlated with gene expression belong to the Clostridiales order. Although this order comprises a very diverse group of bacteria and functional interpretation is complicated, a previous study highlighted the relevance of the Clostridiales in relation to metabolic status in European women [66]. It should be noted that observed correlations between microbiota composition and colonic gene expression cannot reveal causal relationships, but may provide complementary layers of evidence. Therefore, we obtained further insights into functional outcomes that strengthen the evidence for causal relationships and provide plausible explanations for our observations.

Interestingly, levels of chenodeoxycholic acid and two secondary bile acids (derivates of cholic acid and chenodeoxycholic acid), but not cholic acid, were lower in the colonic luminal content of mice on CR

as compared to the other diet groups. These results are in agreement with findings of short-term CR experiments [67]. Elevated levels of secondary bile acids have been associated with inflammation, enhanced intestinal permeability, and colorectal cancer, which highlight the relevance of these compounds for colonic health and involvement in disease development [68-70]. Primary bile acids are synthesised from cholesterol in the liver, while secondary bile acids are formed by the intestinal bacteria [71]. Levels of the identified bile acids in our study were inversely correlated with relative abundance of *Bifidobacterium, Parasutterella* and *Lactobacillus* genera. Although firm conclusions about causal relationships should not be purely based on observed correlations, the intestinal microbiota is thus a plausible candidate that may explain observed differences in bile acid levels across the diet groups. Another explanation for the lowered bile acid levels in the colonic luminal content of mice on CR is based on previous observations that faecal excretion of bile acids is reduced upon CR in obese individuals, which is presumably due to a lowered food mass in the colon [72] or due to more efficient uptake in the ileum [73]. In our study, levels of SCFAs in the colonic luminal content were relatively low, which could be inherent to our semi-synthetic diets low in dietary fibre as compared to regular chow diets.

We have shown that urinary levels of TCA cycle metabolites were increased after lifelong CR as compared to the C or MF diet. Obviously, TCA cycle metabolites in the urine may originate from various tissues and organs, including the colon. Increased expression of genes encoding for metabolic enzymes in the TCA cycle have been previously shown in white adipose tissue of mice under long-term CR [74]. Interestingly, levels of citrate and other TCA metabolites were decreased in livers of old mice that underwent long-term CR [75]. The contradicting findings for liver and urine may point towards specific urinary excretion of TCA cycle intermediates upon an altered energy balance, which is also clearly demonstrated in relation to human adiposity [53]. We also observed lower levels of sucrose in the urine of CR mice as compared to the MF group, which may be due to a 'leaky gut' phenotype in the MF mice [76]. It should be mentioned that in our study urine samples were collected according to strict protocols in the morning, i.e. up to 17 hours after provision of the food [29]. The CR mice tended to consume their fixed portion quickly after provision. This implies that CR mice may have been fasted at the time of urine collection, whereas the C and MF mice had *ad libitum* access to their food and their fasting status may have slightly varied.

The unique diet switch from CR to an *ad libitum* MF diet at the age 24 months is one of the main strengths of our study. This switch allowed thorough examination of persistence of the CR-induced effects upon challenging conditions. Previous studies showed that favourable metabolic effects of CR, such as an improved glucose tolerance, are persistent after discontinuation of prolonged CR [26, 27]. In our study, we have seen that most gene expression profiles, relative abundance of microbial genera and levels of

metabolites adapted to patterns of the MF mice after the diet switch. Our findings are in agreement with results of our previous study focussing on persistence of the liver transcriptome in these mice [33]. Xu and colleagues recently described persistent microbial patterns after switching from CR to a high-fat diet, although it should be noted that their research was performed in the context of a chemically-induced colon cancer model [25]. We showed that expression of 27 genes remained CR-associated. Epigenetic programming may be a plausible explanation for the persistent expression of these genes [77]. Beside some immunoglobulin chains, mucin 20 (*Muc20*) was one of the genes that retained a CR-like profile with lower expression levels as compared to the MF diet. *Muc20* encodes a membrane-bound mucin [78] with low expression levels in the colon. Overexpression of this gene has been associated with a poor clinical outcome in colorectal cancer patients and aggressive colorectal cancer biology [79]. The majority of the differentially expressed genes, specifically involved in lipid metabolism, changed towards expression profiles of the MF mice.

Altogether, this study suggests that prolonged CR may beneficially affect indicators of colonic health in aging mice. A potential mode of action of CR includes prevention of a disturbed colonic microbial ecosystem during aging. Consequently, diminished exposure to specific microbial end-products and components, such as secondary bile acids or lipopolysaccharide (LPS), may result in attenuation of immune cell activation and hence prevention of chronic, low-grade inflammation in the colon (**Figure 7**). Moreover, we have now successfully shown that effects of CR on indicators of colonic health in mice were dynamic and were merely nullified after switching to a diet high in energy, although persistent effects on functional or pathological outcomes cannot be excluded. Our findings provide unique leads for further studies that need to address optimal and feasible strategies for prolonged energy deprivation, with consideration of potential detrimental effects, such as an increased risk of infections or infertility. Naturally, evidence from animal models does not perfectly reflect the human situation [80] and caveats should be carefully considered in terms of feasibility, duration, timing and stringency of the CR conditions [81]. Therefore, it should be further explored how these strategies can be implemented in the human lifestyle and as such may contribute to healthy aging.

ACKNOWLEDGEMENTS

We would like to thank Guido Hooiveld for his valuable suggestions regarding data analysis and Adrià López Nadal and Mark Boekschoten for their technical support.

CONFLICTS OF INTEREST: none

SOURCES OF FUNDING

This work was financially supported by the European Union's Seventh Framework Programme (FP7/2007-2011) IDEAL-aging under grant agreement no 259679. DE Kok was financially supported by a research grant (2011-5234) from the Alpe d'Huzes/Dutch Cancer Society. The funding bodies did not have a role in the design of the study, the collection, analysis and interpretation of data, the decision to publish these findings and writing of the manuscript.

REFERENCES

[1] López-Otín C, Blasco MA, Partridge L, Serrano M, Kroemer G. The Hallmarks of Aging. Cell. 2013;153:1194-217.
[2] Gems D, Partridge L. Genetics of Longevity in Model Organisms: Debates and Paradigm Shifts. Annual Review of Physiology. 2013;75:621-44.
[3] Hung WW, Ross JS, Boockvar KS, Siu AL. Recent trends in chronic disease, impairment and disability among older adults in the United States. BMC geriatrics. 2011;11:47.
[4] Fontana L, Partridge L. Promoting Health and Longevity through Diet: From Model Organisms to Humans. Cell. 2015;161:106-18.
[5] Mattison JA, Colman RJ, Beasley TM, Allison DB, Kemnitz JW, Roth GS, et al. Caloric restriction improves health and survival of rhesus monkeys. Nat Commun. 2017;8:14063.
[6] Most J, Tosti V, Redman LM, Fontana L. Calorie restriction in humans: An update. Ageing Research Reviews. 2017;39:36-45.
[7] Chung KW, Kim DH, Park MH, Choi YJ, Kim ND, Lee J, et al. Recent advances in calorie restriction research on aging. Experimental Gerontology. 2013;48:1049-53.
[8] López-Lluch G, Navas P. Calorie restriction as an intervention in ageing. The Journal of Physiology. 2016;594:2043-60.
[9] Franceschi C, Campisi J. Chronic Inflammation (Inflammaging) and Its Potential Contribution to Age-Associated Diseases. The Journals of Gerontology Series A: Biological Sciences and Medical Sciences. 2014;69:S4-S9.
[10] Chung HY, Kim HJ, Kim JW, Yu BP. The inflammation hypothesis of aging: molecular modulation by calorie restriction. Annals of the New York Academy of Sciences. 2001;928:327-35.
[11] Xia S, Zhang X, Zheng S, Khanabdali R, Kalionis B, Wu J, et al. An Update on Inflamm-Aging: Mechanisms, Prevention, and Treatment. Journal of Immunology Research. 2016;2016:8426874.
[12] Fontana L, Klein S. Aging, adiposity, and calorie restriction. Jama. 2007;297:986-94.
[13] Bales CW, Kraus WE. Caloric restriction: implications for human cardiometabolic health. Journal of cardiopulmonary rehabilitation and prevention. 2013;33:201-8.
[14] Biagi E, Candela M, Fairweather-Tait S, Franceschi C, Brigidi P. Ageing of the human metaorganism: the microbial counterpart. Age. 2012;34:247-67.
[15] Claesson MJ, Jeffery IB, Conde S, Power SE, O'Connor EM, Cusack S, et al. Gut microbiota composition correlates with diet and health in the elderly. Nature. 2012;488:178-84.
[16] Andrade ME, Araujo RS, de Barros PA, Soares AD, Abrantes FA, Generoso Sde V, et al. The role of immunomodulators on intestinal barrier homeostasis in experimental models. Clinical nutrition (Edinburgh, Scotland). 2015;34:1080-7.
[17] Turner JR. Intestinal mucosal barrier function in health and disease. 2009;9:799-809.
[18] Steegenga WT, de Wit NJ, Boekschoten MV, Ijssennagger N, Lute C, Keshtkar S, et al. Structural, functional and molecular analysis of the effects of aging in the small intestine and colon of C57BL/6J mice. BMC medical genomics. 2012;5:38.
[19] Biagi E, Nylund L, Candela M, Ostan R, Bucci L, Pini E, et al. Through ageing, and beyond: gut microbiota and inflammatory status in seniors and centenarians. PLoS One. 2010;5:e10667.
[20] Langille MG, Meehan CJ, Koenig JE, Dhanani AS, Rose RA, Howlett SE, et al. Microbial shifts in the aging mouse gut. Microbiome. 2014;2:50.
[21] Woodmansey EJ, McMurdo ME, Macfarlane GT, Macfarlane S. Comparison of compositions and metabolic activities of fecal microbiotas in young adults and in antibiotic-treated and non-antibiotic-treated elderly subjects. Applied and environmental microbiology. 2004;70:6113-22.
[22] Zhang C, Li S, Yang L, Huang P, Li W, Wang S, et al. Structural modulation of gut microbiota in life-long calorie-restricted mice. Nature communications. 2013;4.
[23] Olivo-Marston SE, Hursting SD, Perkins SN, Schetter A, Khan M, Croce C, et al. Effects of calorie restriction and diet-induced obesity on murine colon carcinogenesis, growth and inflammatory factors, and microRNA expression. PLoS One. 2014;9:e94765.
[24] Harvey AE, Lashinger LM, Otto G, Nunez NP, Hursting SD. Decreased systemic IGF-1 in response to calorie restriction modulates murine tumor cell growth, nuclear factor-kappaB activation, and inflammation-related gene expression. Molecular carcinogenesis. 2013;52:997-1006.
[25] Xu J, Galley JD, Bailey MT, Thomas-Ahner JM, Clinton SK, Olivo-Marston SE. The Impact of Dietary Energy Intake Early in Life on the Colonic Microbiota of Adult Mice. Scientific reports. 2016;6:19083.

[26] Selman C, Hempenstall S. Evidence of a metabolic memory to early-life dietary restriction in male C57BL/6 mice. Longevity & Healthspan. 2012;1:2-.
[27] Cameron KM, Miwa S, Walker C, von Zglinicki T. Male mice retain a metabolic memory of improved glucose tolerance induced during adult onset, short-term dietary restriction. Longevity & Healthspan. 2012;1:3-.
[28] Rusli F, Boekschoten MV, Zubia AA, Lute C, Muller M, Steegenga WT. A weekly alternating diet between caloric restriction and medium fat protects the liver from fatty liver development in middle-aged C57BL/6J mice. Molecular nutrition & food research. 2015;59:533-43.
[29] van Norren K, Rusli F, van Dijk M, Lute C, Nagel J, Dijk FJ, et al. Behavioural changes are a major contributing factor in the reduction of sarcopenia in caloric-restricted ageing mice. Journal of cachexia, sarcopenia and muscle. 2015;6:253-68.
[30] Rusli F, Deelen J, Andriyani E, Boekschoten MV, Lute C, van den Akker EB, et al. Fibroblast growth factor 21 reflects liver fat accumulation and dysregulation of signalling pathways in the liver of C57BL/6J mice. Scientific reports. 2016;6:30484.
[31] Szalowska E, Tesfay HA, van Hijum SA, Kersten S. Transcriptomic signatures of peroxisome proliferator-activated receptor alpha (PPARalpha) in different mouse liver models identify novel aspects of its biology. BMC genomics. 2014;15:1106.
[32] Georgiadi A, Boekschoten MV, Müller M, Kersten S. Detailed transcriptomics analysis of the effect of dietary fatty acids on gene expression in the heart. Physiological Genomics. 2012;44:352-61.
[33] Rusli F, Boekschoten MV, Borelli V, Sun C, Lute C, Menke AL, et al. Plasticity of life-long calorie restricted C57BL/6J mice in adapting to a medium-fat diet intervention at old age - Aging Cell (in press). 2017.
[34] Irizarry RA, Hobbs B, Collin F, Beazer-Barclay YD, Antonellis KJ, Scherf U, et al. Exploration, normalization, and summaries of high density oligonucleotide array probe level data. Biostatistics (Oxford, England). 2003;4:249-64.
[35] Dai M, Wang P, Boyd AD, Kostov G, Athey B, Jones EG, et al. Evolving gene/transcript definitions significantly alter the interpretation of GeneChip data. Nucleic acids research. 2005;33:e175.
[36] Sartor MA, Tomlinson CR, Wesselkamper SC, Sivaganesan S, Leikauf GD, Medvedovic M. Intensity-based hierarchical Bayes method improves testing for differentially expressed genes in microarray experiments. BMC bioinformatics. 2006;7:538.
[37] Quast C, Pruesse E, Yilmaz P, Gerken J, Schweer T, Yarza P, et al. The SILVA ribosomal RNA gene database project: improved data processing and web-based tools. Nucleic acids research. 2013;41:D590-D6.
[38] C.J.F. tB, Lepš J. Canoco 5: Canoco reference manual and user's guide: software for ordination (version 5). Microcomputer Power (Ithaca, NY, USA) 496 pp.2012.
[39] Legendre P, Gallagher ED. Ecologically meaningful transformations for ordination of species data. Oecologia. 2001;129:271-80.
[40] Haenen D, Souza da Silva C, Zhang J, Koopmans SJ, Bosch G, Vervoort J, et al. Resistant starch induces catabolic but suppresses immune and cell division pathways and changes the microbiome in the proximal colon of male pigs. The Journal of nutrition. 2013;143:1889-98.
[41] Laghi L, Picone G, Cruciani F, Brigidi P, Calanni F, Donders G, et al. Rifaximin modulates the vaginal microbiome and metabolome in women affected by bacterial vaginosis. Antimicrobial agents and chemotherapy. 2014;58:3411-20.
[42] Coombes KR, Fritsche HA, Jr., Clarke C, Chen JN, Baggerly KA, Morris JS, et al. Quality control and peak finding for proteomics data collected from nipple aspirate fluid by surface-enhanced laser desorption and ionization. Clinical chemistry. 2003;49:1615-23.
[43] Liland KH, Almoy T, Mevik BH. Optimal choice of baseline correction for multivariate calibration of spectra. Applied spectroscopy. 2010;64:1007-16.
[44] Savorani F, Tomasi G, Engelsen SB. icoshift: A versatile tool for the rapid alignment of 1D NMR spectra. Journal of magnetic resonance (San Diego, Calif : 1997). 2010;202:190-202.
[45] Dieterle F, Ross A, Schlotterbeck G, Senn H. Probabilistic Quotient Normalization as Robust Method to Account for Dilution of Complex Biological Mixtures. Application in 1H NMR Metabonomics. Analytical chemistry. 2006;78:4281-90.
[46] Wishart DS, Tzur D, Knox C, Eisner R, Guo AC, Young N, et al. HMDB: the Human Metabolome Database. Nucleic acids research. 2007;35:D521-6.
[47] Gonzalez I, Cao KA, Davis MJ, Dejean S. Visualising associations between paired 'omics' data sets. BioData mining. 2012;5:19.
[48] Fernandes AD, Reid JNS, Macklaim JM, McMurrough TA, Edgell DR, Gloor GB. Unifying the analysis of high-throughput sequencing datasets: characterizing RNA-seq, 16S rRNA gene sequencing and selective growth experiments by compositional data analysis. Microbiome. 2014;2:15-.
[49] Kuleshov MV, Jones MR, Rouillard AD, Fernandez NF, Duan Q, Wang Z, et al. Enrichr: a comprehensive gene set enrichment analysis web server 2016 update. Nucleic acids research. 2016.
[50] Chen EY, Tan CM, Kou Y, Duan Q, Wang Z, Meirelles GV, et al. Enrichr: interactive and collaborative HTML5 gene list enrichment analysis tool. BMC bioinformatics. 2013;14:128.
[51] Shannon P, Markiel A, Ozier O, Baliga NS, Wang JT, Ramage D, et al. Cytoscape: a software environment for integrated models of biomolecular interaction networks. Genome Res. 2003;13:2498-504.
[52] Gowda GA, Ijare OB, Somashekar BS, Sharma A, Kapoor VK, Khetrapal CL. Single-step analysis of individual conjugated bile acids in human bile using 1H NMR spectroscopy. Lipids. 2006;41:591-603.
[53] Elliott P, Posma JM, Chan Q, Garcia-Perez I, Wijeyesekera A, Bictash M, et al. Urinary metabolic signatures of human adiposity. Science Translational Medicine. 2015;7:285ra62-ra62.
[54] Nikolich-Žugich J, Messaoudi I. Mice and flies and monkeys too: Caloric restriction rejuvenates the aging immune system of non-human primates. Experimental Gerontology. 2005;40:884-93.
[55] Franceschi C, Capri M, Monti D, Giunta S, Olivieri F, Sevini F, et al. Inflammaging and anti-inflammaging: a systemic perspective on aging and longevity emerged from studies in humans. Mechanisms of ageing and development. 2007;128:92-105.

[56] Lee C-K, Allison DB, Brand J, Weindruch R, Prolla TA. Transcriptional profiles associated with aging and middle age-onset caloric restriction in mouse hearts. Proceedings of the National Academy of Sciences. 2002;99:14988-93.
[57] Farazi M, Nguyen J, Goldufsky J, Linnane S, Lukaesko L, Weinberg AD, et al. Caloric restriction maintains OX40 agonist-mediated tumor immunity and CD4 T cell priming during aging. Cancer immunology, immunotherapy : CII. 2014;63:615-26.
[58] Kim KA, Jeong JJ, Yoo SY, Kim DH. Gut microbiota lipopolysaccharide accelerates inflamm-aging in mice. BMC Microbiol. 2016;16:9.
[59] Jeong J-J, Kim K-A, Jang S-E, Woo J-Y, Han MJ, Kim D-H. Orally Administrated Lactobacillus pentosus var. plantarum C29 Ameliorates Age-Dependent Colitis by Inhibiting the Nuclear Factor-Kappa B Signaling Pathway via the Regulation of Lipopolysaccharide Production by Gut Microbiota. PLoS ONE. 2015;10:e0116533.
[60] Thevaranjan N, Puchta A, Schulz C, Naidoo A, Szamosi JC, Verschoor CP, et al. Age-Associated Microbial Dysbiosis Promotes Intestinal Permeability, Systemic Inflammation, and Macrophage Dysfunction. Cell host & microbe. 2017;21:455-66.e4.
[61] Odamaki T, Kato K, Sugahara H, Hashikura N, Takahashi S, Xiao JZ, et al. Age-related changes in gut microbiota composition from newborn to centenarian: a cross-sectional study. BMC Microbiol. 2016;16:90.
[62] Wu BB, Yang Y, Xu X, Wang WP. Effects of Bifidobacterium supplementation on intestinal microbiota composition and the immune response in healthy infants. World journal of pediatrics : WJP. 2016;12:177-82.
[63] Riviere A, Selak M, Lantin D, Leroy F, De Vuyst L. Bifidobacteria and Butyrate-Producing Colon Bacteria: Importance and Strategies for Their Stimulation in the Human Gut. Frontiers in microbiology. 2016;7:979.
[64] Maukonen J, Kolho KL, Paasela M, Honkanen J, Klemetti P, Vaarala O, et al. Altered Fecal Microbiota in Paediatric Inflammatory Bowel Disease. Journal of Crohn's & colitis. 2015;9:1088-95.
[65] Claus SP, Ellero SL, Berger B, Krause L, Bruttin A, Molina J, et al. Colonization-Induced Host-Gut Microbial Metabolic Interaction. mBio. 2011;2:e00271-10.
[66] Karlsson FH, Tremaroli V, Nookaew I, Bergstrom G, Behre CJ, Fagerberg B, et al. Gut metagenome in European women with normal, impaired and diabetic glucose control. 2013;498:99-103.
[67] Fu ZD, Klaassen CD. Increased bile acids in enterohepatic circulation by short-term calorie restriction in male mice. Toxicology and Applied Pharmacology. 2013;273:680-90.
[68] Nagengast FM, Grubben MJ, van Munster IP. Role of bile acids in colorectal carcinogenesis. European journal of cancer (Oxford, England : 1990). 1995;31a:1067-70.
[69] Duboc H, Rajca S, Rainteau D, Benarous D, Maubert MA, Quervain E, et al. Connecting dysbiosis, bile-acid dysmetabolism and gut inflammation in inflammatory bowel diseases. Gut. 2013;62:531-9.
[70] Murakami Y, Tanabe S, Suzuki T. High-fat Diet-induced Intestinal Hyperpermeability is Associated with Increased Bile Acids in the Large Intestine of Mice. Journal of food science. 2016;81:H216-22.
[71] Kuipers F, Bloks VW, Groen AK. Beyond intestinal soap--bile acids in metabolic control. Nature reviews Endocrinology. 2014;10:488-98.
[72] Straniero S, Rosqvist F, Edholm D, Ahlstrom H, Kullberg J, Sundbom M, et al. Acute caloric restriction counteracts hepatic bile acid and cholesterol deficiency in morbid obesity. Journal of internal medicine. 2017;281:507-17.
[73] Dumaswala R, Berkowitz D, Setchell KD, Heubi JE. Effect of fasting on the enterohepatic circulation of bile acids in rats. The American journal of physiology. 1994;267:G836-42.
[74] Higami Y, Pugh TD, Page GP, Allison DB, Prolla TA, Weindruch R. Adipose tissue energy metabolism: altered gene expression profile of mice subjected to long-term caloric restriction. FASEB journal : official publication of the Federation of American Societies for Experimental Biology. 2004;18:415-7.
[75] Hagopian K, Ramsey JJ, Weindruch R. Krebs cycle enzymes from livers of old mice are differentially regulated by caloric restriction. Experimental Gerontology. 2004;39:1145-54.
[76] Meddings JB, Sutherland LR, Byles NI, Wallace JL. Sucrose: a novel permeability marker for gastroduodenal disease. Gastroenterology. 1993;104:1619-26.
[77] Yu DH, Gadkari M, Zhou Q, Yu S, Gao N, Guan Y, et al. Postnatal epigenetic regulation of intestinal stem cells requires DNA methylation and is guided by the microbiome. Genome biology. 2015;16:211.
[78] Andrianifahanana M, Moniaux N, Batra SK. Regulation of mucin expression: Mechanistic aspects and implications for cancer and inflammatory diseases. Biochimica et Biophysica Acta (BBA) - Reviews on Cancer. 2006;1765:189-222.
[79] Xiao X, Wang L, Wei P, Chi Y, Li D, Wang Q, et al. Role of MUC20 overexpression as a predictor of recurrence and poor outcome in colorectal cancer. Journal of Translational Medicine. 2013;11:151-.
[80] Ingram DK, de Cabo R. Calorie restriction in rodents: Caveats to consider. Ageing Research Reviews. 2017;39:15-28.
[81] Fontana L. The science of nutritional modulation of aging. Ageing Research Reviews. 2017;39:1-2.

FIGURE LEGENDS

Figure 1: Gene expression analyses in colonic scrapings of mice fed different dietary regimens. Mice were lifelong fed a control diet (C), calorie restricted diet (CR) or moderate-fat diet (MF) and sacrificed at 6 or 28 months of age. A subgroup of mice switched from the CR to MF diet at 24 months (CR>MF). **[A]** The number of differentially expressed genes for comparisons of the respective dietary regimens based on an IBMT p-value <0.01. **[B]** The top-5 canonical pathways that were differentially regulated in mice fed the CR diet versus the MF diet at 6 (black) and 28 months (grey) of age. The numbers behind the pathways represent the total number of genes, whereas the numbers behind de bars reflect the number of differentially expressed genes (p-value <0.01). **[C]** The overlap between up-, and down-regulated genes that were differentially expressed between the CR diet versus the MF diet at 6 and 28 months. **[D]** Mean plasma levels of interleukin 6 (Il6). * p<0.05 and ** p<0.01 in 1-way ANOVA followed by Tukey's test. **[E]** Principal component analysis plot showing the distribution of the individual mice based on the expression of the 1000 most variable genes at 28 months. **[F]** Identification of genes that remained similar to the CR-profile or switched towards the MF-profile after the diet switch (CR>MF). **[G]** Mean microarray expression levels for *Muc20* in the colonic scrapings. **[H]** Mean microarray expression levels for *Scd1* in the colonic scrapings. For all panels: presented error bars reflect standard error of the mean (SEM). Number of mice for the gene expression experiments at 6 months: (C) n=4, (CR) n=6, (MF) n=5 and at 28 months: (C) n=7, (CR) n=6, (MF) n=7, (CR>MF) n=7.

Figure 2: Microbiota composition in the colonic luminal content. [A] Alpha-diversities as indicated by the Shannon entropy for mice fed the control diet (C), moderate-fat diet (MF), calorie restricted diet (CR) at 6 and 28 months of age. Also mice exposed to CR for 24 months and subsequently switched to the MF diet (CR>MF) are presented. Box and whiskers represent mean and min-max, respectively. **[B]** Relative abundance at the phylum level. **[C]** Principal Coordinates Analysis (PCoA) plot based on the Bray Curtis distances showing the dissimilarity of the samples based on microbiota composition at the OTU level **[D]** Heatmap showing the relative abundance for the 26 genera that were identified through a Kruskal Wallis test (p<0.05 with Bonferroni correction, all groups). The genera indicated with an asterisk (*) also showed a significant contrast for the dietary regimens within an age category (Dunn's post hoc analyses, p<0.05). **[E]** Schematic overview of the most pronounced genera that were enriched or depleted in the mice on CR. The age-independent category refers to similar enrichment or depletion of genera at young and old age, whereas the age-dependent category describes aging-related effects that were diminished upon CR exposure. **[F]** Correlation of body weight at sacrifice and relative abundance of the *Bifidobacterium* genus in the colonic luminal content. Shapes and colours indicate young (square, 6 months) or old (triangle, 28

months) mice upon the C (black), CR (blue), MF (red) diets or the diet switch CR>MF (green). All diet groups were based on n=10 mice, except for the MF group at 28 months which consisted of n=7 mice.

Figure 3: Redundancy analysis of colonic microbial profiles. Redundancy analysis (RDA) showing the microbial profiles in the colonic luminal content for the respective age and diet groups based on the individual OTUs with a relative abundance of ≥0.1% in at least 1 sample. **[A]** Sample plot showing the clustering of the samples. Squares (young) and triangles (old) represent individual mice and large triangles are representative for group means. **[B]** Biplot showing the 25 OTUs (arrows) for which the observed variation is best explained by the explanatory variables (diet groups), and the mean scores for the diet groups (triangles). Percentages on the first and second ordination axes indicate the explained variation in the dataset (16% and 8%, respectively). All diet groups were based on n=10 mice, except for the MF group at 28 months which consisted of n=7 mice.

Figure 4: Microbial genera in the colonic luminal content associated with gene expression in the colon. [A] Heatmap showing the correlation for the relative abundance of 56 genera and the expression of 1000 most variable genes at the age of 28 months. The two datasets were integrated based on a partial least square (PLS) analysis in the canonical mode. Hierarchical clustering based on the Euclidian distance was applied for the identification of the main clusters for both genes (1-6) and genera (A-F). **[B]** Relevance network showing the genera (grey octagons) and genes (white squares). Only edges with a pairwise association measure <-0.75 (blue) or >0.75 (red) were presented.

Figure 5: Metabolite profiles in the colonic luminal content. ^{1}H-NMR data of the colonic luminal content for mice at 6 and 28 months of age who were lifelong fed a control diet (C), calorie restricted diet (CR) or moderate-fat diet (MF) or switched from CR to MF at 24 months of age (CR>MF). Analysis of metabolite levels (presented as mean ± SEM) is based on n=6-8 mice per group. Comparisons between groups were made using Kruskal Wallis tests followed by Dunn's post hoc tests restricted to comparisons within the age categories (*p<0.05 and **p<0.01) **[A]** acetate, **[B]** butyrate, **[C]** propionate, **[D]** succinate, **[E]** cholic acid (CA), **[F]** deoxycholic acid (DxCA) or taurodeoxycholic acid (TDxCA), **[G]** chendeoxycholic acid (ChDxCA), **[H]** chendeoxycholic acid (ChDxCA) derivate, **[I]** Heatmap showing the Spearman correlation for the integrals of the identified bile acids and relative abundance of 69 microbial genera. Only genera showing a Spearman r>0.5 are included in this heatmap. Correlation analyses based on 45 mice (n=6-8 per group) for which both metabolomic as well as microbial data were available.

Figure 6: Metabolite profiles in the urine. [A] Loading plot showing the urinary metabolites (n=58) contributing to the discrimination of the three diet groups based on a partial least square discriminant analyses (PLS-DA). The corresponding score plot is presented in panel C. **[B]** Simplified heatmap showing the log-ratio for the concentrations of the urinary metabolites in mice fed the CR versus MF diet. Concentrations of the molecules were log2 transformed and the log-ratio (CR minus MF) was calculated to express the difference between the two groups. Only log-ratios of <-1 or >1 (corresponding to a fold change of 2) were illustrated in this panel. **[C]** Score plot showing the supervised clustering of the individual mice along the three diet groups based on the PLS-DA. **[D]** Unsupervised clustering of the mice according to their urinary metabolites was visualized in a principal component analyses (PCA) score plot. **[E]** and **[F]** Levels (mean ± SEM) of citrate and 2-hydroxyisobutyrate in the urine of mice in the three diet groups. ** represent a p-value <0.01 for the Dunn's tests which were performed after a Kruskal Wallis test with a p-value of <0.01. Analyses based on n=7-9 mice per diet group. Black circles represent the C diet, blue circles the CR diet and red circles the MF diet.

Figure 7: Hypothetical model describing effects of calorie restriction on indicators of colonic health in aging mice. Based on the results of the current study, it has been hypothesized that calorie restriction is able to maintain colonic homeostasis through stabilization of microbiota composition (symbiosis) during aging. Diminished exposure to specific microbial end-products and components, such as secondary bile acids or lipopolysaccharide (LPS), may result in attenuation of immune cell activation and hence prevention of chronic, low-grade inflammation in the colon.

Table 1: Differentially regulated genes in the colonic scrapings for the comparison of calorie restriction and the moderate-fat diet

Gene	Description	Fold change	p-value
Up-regulation with CR at the age of 28 months			
Igkv2-112	immunoglobulin kappa variable 2-112	4.2	6.2E-03
Scd1	stearoyl-Coenzyme A desaturase 1	3.9	1.7E-08
Car3	carbonic anhydrase 3	3.3	3.1E-03
Cyp2e1	cytochrome P450, family 2, subfamily e, polypeptide 1	3.1	1.7E-03
Akr1c18	aldo-keto reductase family 1, member C18	2.3	3.8E-03
Me1	malic enzyme 1, NADP(+)-dependent, cytosolic	2.0	1.4E-03
Lpl	lipoprotein lipase	1.8	1.0E-04
Mal	myelin and lymphocyte protein, T cell differentiation protein	1.8	5.3E-03
Thrsp	thyroid hormone responsive	1.7	8.8E-04
LOC102638466	uncharacterized LOC102638466	1.5	6.6E-05
Ddx43	DEAD (Asp-Glu-Ala-Asp) box polypeptide 43	1.5	4.3E-03
D930020B18Rik	RIKEN cDNA D930020B18 gene	1.5	2.8E-03
Aldh1a1	aldehyde dehydrogenase family 1, subfamily A1	1.4	1.3E-03
Olfr920	olfactory receptor 920	1.4	2.1E-03
Fads1	fatty acid desaturase 1	1.4	1.6E-04
Irs2	insulin receptor substrate 2	1.4	3.9E-04
Olfr829	olfactory receptor 829	1.4	8.8E-03
Acox2	acyl-Coenzyme A oxidase 2, branched chain	1.4	1.8E-03
Brca2	breast cancer 2	1.4	9.7E-05
Ms4a10	membrane-spanning 4-domains, subfamily A, member 10	1.4	2.5E-03
Down-regulation with CR at the age of 28 months			
Ighv8-12	immunoglobulin heavy variable V8-12	-4.9	2.9E-03
Igkv8-24	immunoglobulin kappa chain variable 8-24	-4.5	2.3E-03
Ighv3-5	immunoglobulin heavy variable 3-5	-3.9	2.8E-03
S100g	S100 calcium binding protein G	-3.8	1.3E-04
Igkv1-135	immunoglobulin kappa variable 1-135	-3.3	9.0E-03
Ighv3-8	immunoglobulin heavy variable V3-8	-3.2	8.3E-03
Ighm	immunoglobulin heavy constant mu	-3.2	1.3E-05
Ighg2c	immunoglobulin heavy constant gamma 2C	-3.0	1.5E-04
Ang4	angiogenin, ribonuclease A family, member 4	-2.8	8.0E-03
Slc30a10	solute carrier family 30, member 10	-2.7	3.7E-07
Ighg2b	immunoglobulin heavy constant gamma 2B	-2.5	5.4E-04
Lyz1	lysozyme 1	-2.4	5.6E-04
Cd79b	CD79B antigen	-2.3	7.4E-03
Cd79a	CD79A antigen	-2.3	4.1E-03
Igkv4-57	immunoglobulin kappa variable 4-57	-2.2	4.7E-03
Retnlb	resistin like beta	-2.2	3.2E-03
Igkv6-20	immunoglobulin kappa variable 6-20	-2.1	7.8E-03
H2-Eb2	histocompatibility 2, class II antigen E beta2	-2.1	6.5E-03
Nox1	NADPH oxidase 1	-2.0	2.4E-04
H2-DMb2	histocompatibility 2, class II, locus Mb2	-2.0	5.9E-03

Top-20 differentially regulated genes identified based on the comparison of gene expression for calorie restriction (CR) and the moderate-fat diet at 28 months of age. The top-20 genes were sorted based on fold changes. Fold changes represent the comparison between calorie restriction (n=6 mice) and the moderate-fat diet (n=7 mice) at the age of 28 months. Only genes with an IBMT p-value <0.01 were considered.

Table 2: Biological annotation for correlated gene and microbiota clusters

	GO term[a]	Adjusted p-value[b]	Z-score	Combined Z-score	Overlapping genes[c]
Gene cluster 2 (181 genes)					
Muscle contraction	0006936	2.45E-06	-2.66	34.41	10/85
Cellular calcium ion homeostasis	0006874	4.30E-04	-3.20	24.77	7/65
Lymphocyte chemotaxis	0048247	4.30E-04	-2.41	18.69	5/25
Neutrophil chemotaxis	0030593	5.04E-04	-2.81	21.35	6/51
Positive regulation of GTPase activity	0043547	5.04E-04	-2.75	20.88	8/112
Gene cluster 3 (152 genes)					
B cell receptor signaling pathway	0050853	1.53E-05	-2.64	29.28	8/67
humoral immune response	0006959	2.69E-04	-3.81	31.34	6/47
T-helper 17 cell lineage commitment	0072540	1.05E-03	-2.77	19.04	3/6
respiratory burst	0045730	4.23E-03	-3.38	18.48	3/10
B cell proliferation	0042100	4.23E-03	-2.31	12.62	4/28

Microbiota	**Members (genera)**	**Phylum**	**Order**
Microbiota cluster D (9 genera)	*Turicibacter*	Firmicutes	Erysipelotrichales
	Clostridium sensu stricto 1	Firmicutes	Clostridiales
	Lachnospiraceae uncultured	Firmicutes	Clostridiales
	Roseburia	Firmicutes	Clostridiales
	Ruminococcaceae incertae sedis	Firmicutes	Clostridiales
	Ruminococcaceae uncultured	Firmicutes	Clostridiales
	Defluviitaleaceae incertae sedis	Firmicutes	Clostridiales
	Peptostreptococcaceae.uncultured	Firmicutes	Clostridiales
	Bilophila	Proteobacteria	Desulfovibrionales
Microbiota cluster F (8 genera)	*Bifidobacterium*	Actinobacteria	Bifidobacteriales
	Coriobacteriaceae uncultured	Actinobacteria	Coriobacteriales
	Parasutterella	Proteobacteria	Burkholderiales
	Lactococcus	Firmicutes	Lactobacillales
	Lactobacillus	Firmicutes	Lactobacillales
	Planomicrobium	Firmicutes	Bacillales
	Catenibacterium	Firmicutes	Erysipelotrichales
	Allobaculum	Firmicutes	Erysipelotrichales

Results for the canonical correlation analyses based on the 1000 genes with most variable expression at old age and 56 genera identified in the colonic luminal content **a)** Gene ontology (GO) biological processes characterizing the gene clusters most pronouncedly correlated to microbiota composition in the colonic luminal content. When more than 5 biological processes were identified, only the top-5 (based on adjusted p-value) was shown. **b)** The adjusted p-value was corrected for multiple testing using the Benjamini-Hochberg method. **c)** The overlapping genes represent the number of genes identified in the analyses relative to the total number of genes annotated to a biological process.

Figure 1

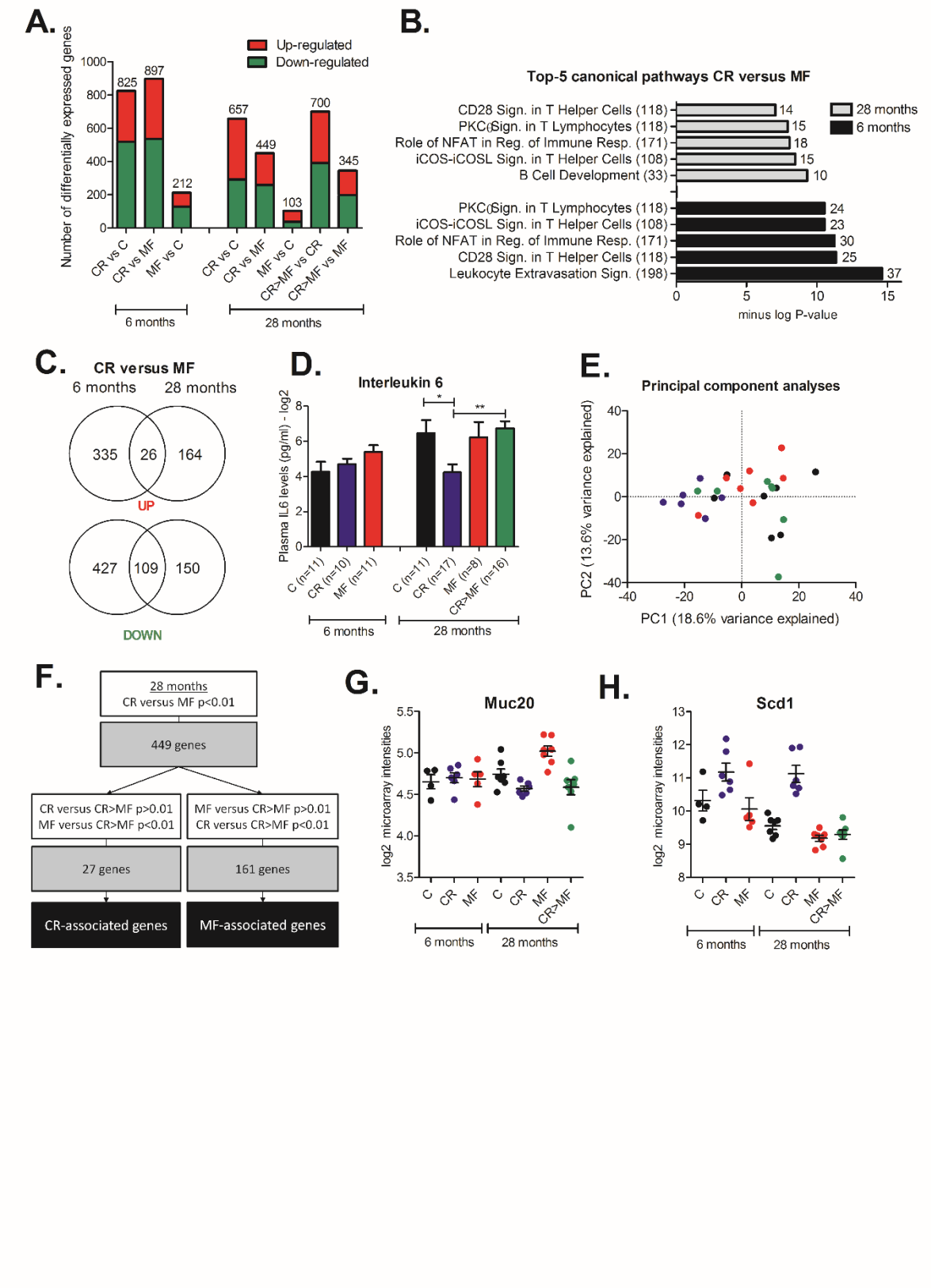

A.
Number of differentially expressed genes
Up-regulated
Down-regulated
825
897
212
657
449
103
700
345
CR vs C
CR vs MF
MF vs C
CR vs C
CR vs MF
MF vs C
CR>MF vs CR
CR>MF vs MF
6 months
28 months
B.
Top-5 canonical pathways CR versus MF
CD28 Sign. in T Helper Cells (118)
PKCθ Sign. in T Lymphocytes (118)
Role of NFAT in Reg. of Immune Resp. (171)
iCOS-iCOSL Sign. in T Helper Cells (108)
B Cell Development (33)
14
15
18
15
10
28 months
6 months
PKCθ Sign. in T Lymphocytes (118)
iCOS-iCOSL Sign. in T Helper Cells (108)
Role of NFAT in Reg. of Immune Resp. (171)
CD28 Sign. in T Helper Cells (118)
Leukocyte Extravasation Sign. (198)
24
23
30
25
37
minus log P-value
C.
CR versus MF
6 months
28 months
335
26
164
UP
427
109
150
DOWN
D.
Interleukin 6
Plasma IL6 levels (pg/ml) - log2
C (n=11)
CR (n=10)
MF (n=11)
C (n=11)
CR (n=17)
MF (n=8)
CR>MF (n=16)
6 months
28 months
E.
Principal component analyses
PC2 (13.6% variance explained)
PC1 (18.6% variance explained)
F.
28 months
CR versus MF p<0.01
449 genes
CR versus CR>MF p>0.01
MF versus CR>MF p<0.01
MF versus CR>MF p>0.01
CR versus CR>MF p<0.01
27 genes
161 genes
CR-associated genes
MF-associated genes
G.
Muc20
log2 microarray intensities
C
CR
MF
C
CR
MF
CR>MF
6 months
28 months
H.
Scd1
log2 microarray intensities
C
CR
MF
C
CR
MF
CR>MF
6 months
28 months

Figure 2

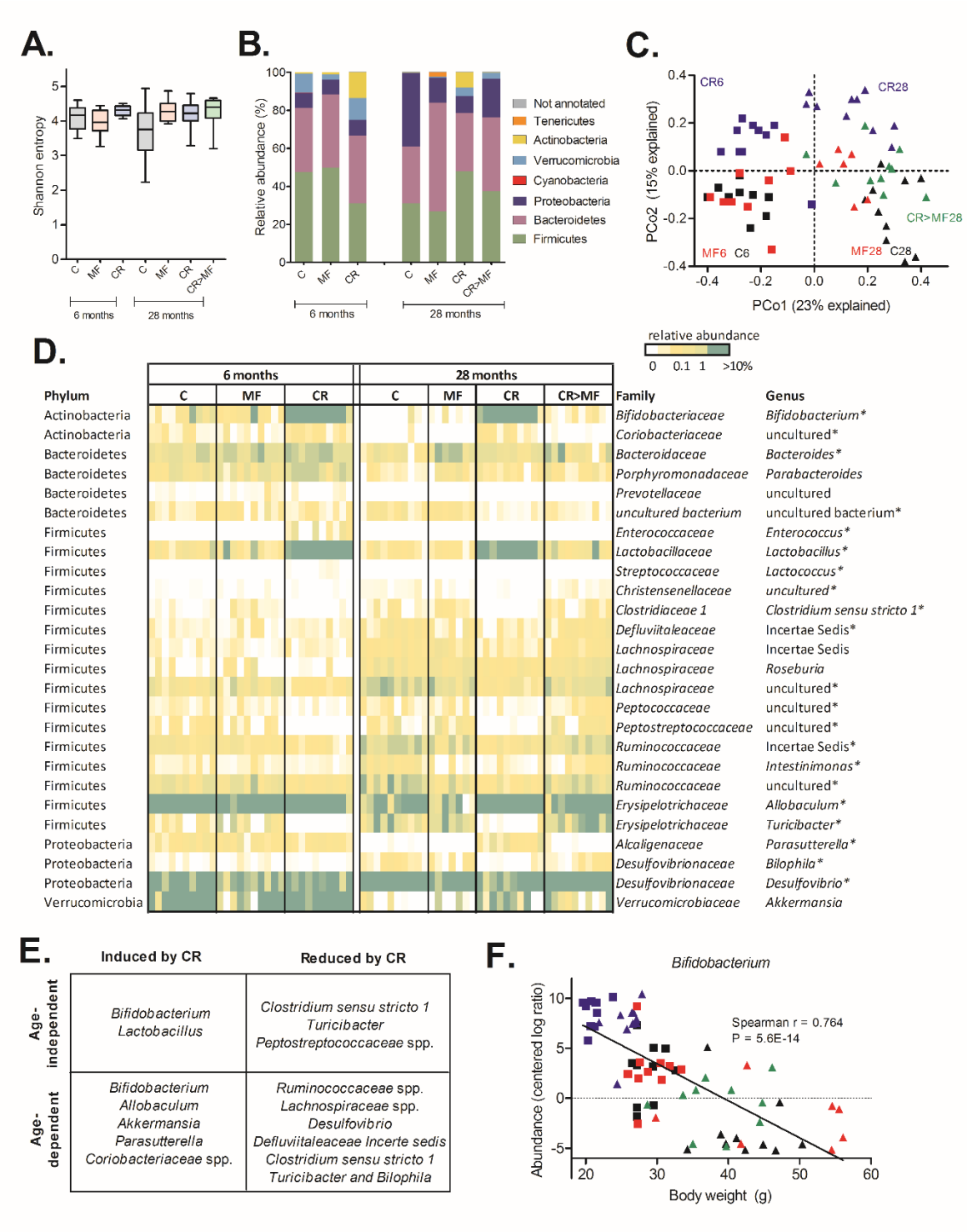

A.
Shannon entropy
C MF CR C MF CR CR>MF
6 months
28 months
B.
Relative abundance (%)
Not annotated
Tenericutes
Actinobacteria
Verrucomicrobia
Cyanobacteria
Proteobacteria
Bacteroidetes
Firmicutes
C MF CR C MF CR CR>MF
6 months
28 months
C.
PCo2 (15% explained)
PCo1 (23% explained)
CR6
CR28
CR>MF28
MF6 C6
MF28 C28
D.
relative abundance
0 0.1 1 >10%
6 months
28 months
Phylum
C MF CR C MF CR CR>MF
Family
Genus
Actinobacteria Bifidobacteriaceae Bifidobacterium*
Actinobacteria Coriobacteriaceae uncultured*
Bacteroidetes Bacteroidaceae Bacteroides*
Bacteroidetes Porphyromonadaceae Parabacteroides
Bacteroidetes Prevotellaceae uncultured
Bacteroidetes uncultured bacterium uncultured bacterium*
Firmicutes Enterococcaceae Enterococcus*
Firmicutes Lactobacillaceae Lactobacillus*
Firmicutes Streptococcaceae Lactococcus*
Firmicutes Christensenellaceae uncultured*
Firmicutes Clostridiaceae 1 Clostridium sensu stricto 1*
Firmicutes Defluviitaleaceae Incertae Sedis*
Firmicutes Lachnospiraceae Incertae Sedis
Firmicutes Lachnospiraceae Roseburia
Firmicutes Lachnospiraceae uncultured*
Firmicutes Peptococcaceae uncultured*
Firmicutes Peptostreptococcaceae uncultured*
Firmicutes Ruminococcaceae Incertae Sedis*
Firmicutes Ruminococcaceae Intestinimonas*
Firmicutes Ruminococcaceae uncultured*
Firmicutes Erysipelotrichaceae Allobaculum*
Firmicutes Erysipelotrichaceae Turicibacter*
Proteobacteria Alcaligenaceae Parasutterella*
Proteobacteria Desulfovibrionaceae Bilophila*
Proteobacteria Desulfovibrionaceae Desulfovibrio*
Verrucomicrobia Verrucomicrobiaceae Akkermansia
E.
Induced by CR
Reduced by CR
Age-independent
Bifidobacterium
Lactobacillus
Clostridium sensu stricto 1
Turicibacter
Peptostreptococcaceae spp.
Age-dependent
Bifidobacterium
Allobaculum
Akkermansia
Parasutterella
Coriobacteriaceae spp.
Ruminococcaceae spp.
Lachnospiraceae spp.
Desulfovibrio
Defluviitaleaceae Incerte sedis
Clostridium sensu stricto 1
Turicibacter and Bilophila
F.
Bifidobacterium
Abundance (centered log ratio)
Spearman r = 0.764
P = 5.6E-14
Body weight (g)

Figure 3

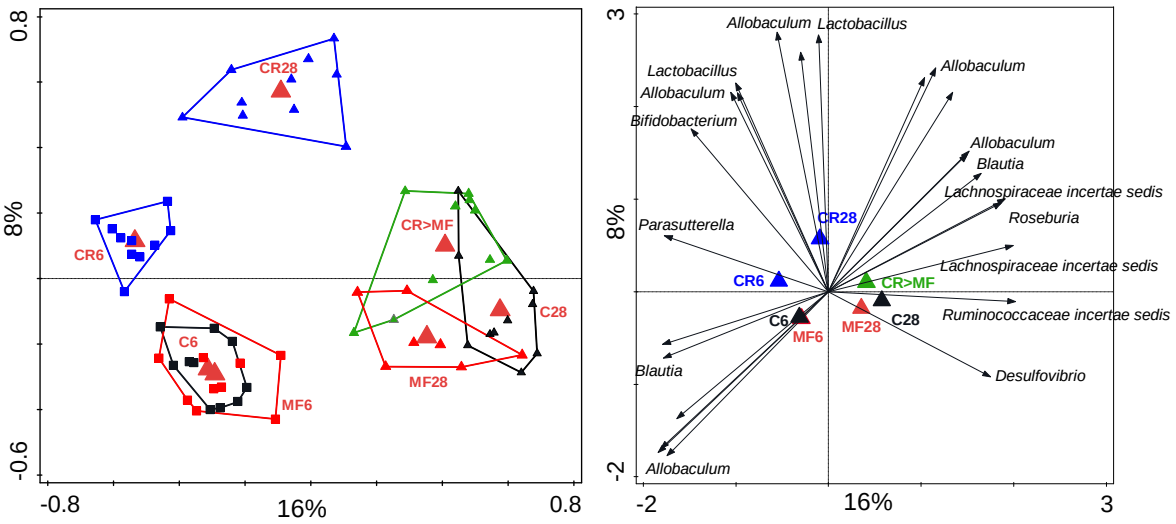

0.8
8%
-0.6
-0.8
16%
0.8
CR28
CR6
CR>MF
C28
C6
MF6
MF28
3
8%
-2
-2
16%
3
Allobaculum
Lactobacillus
Lactobacillus
Allobaculum
Bifidobacterium
Allobaculum
Allobaculum
Blautia
Lachnospiraceae incertae sedis
Roseburia
Parasutterella
CR28
Lachnospiraceae incertae sedis
CR6
CR>MF
C6
MF6
MF28
C28
Ruminococcaceae incertae sedis
Blautia
Desulfovibrio
Allobaculum

Figure 4

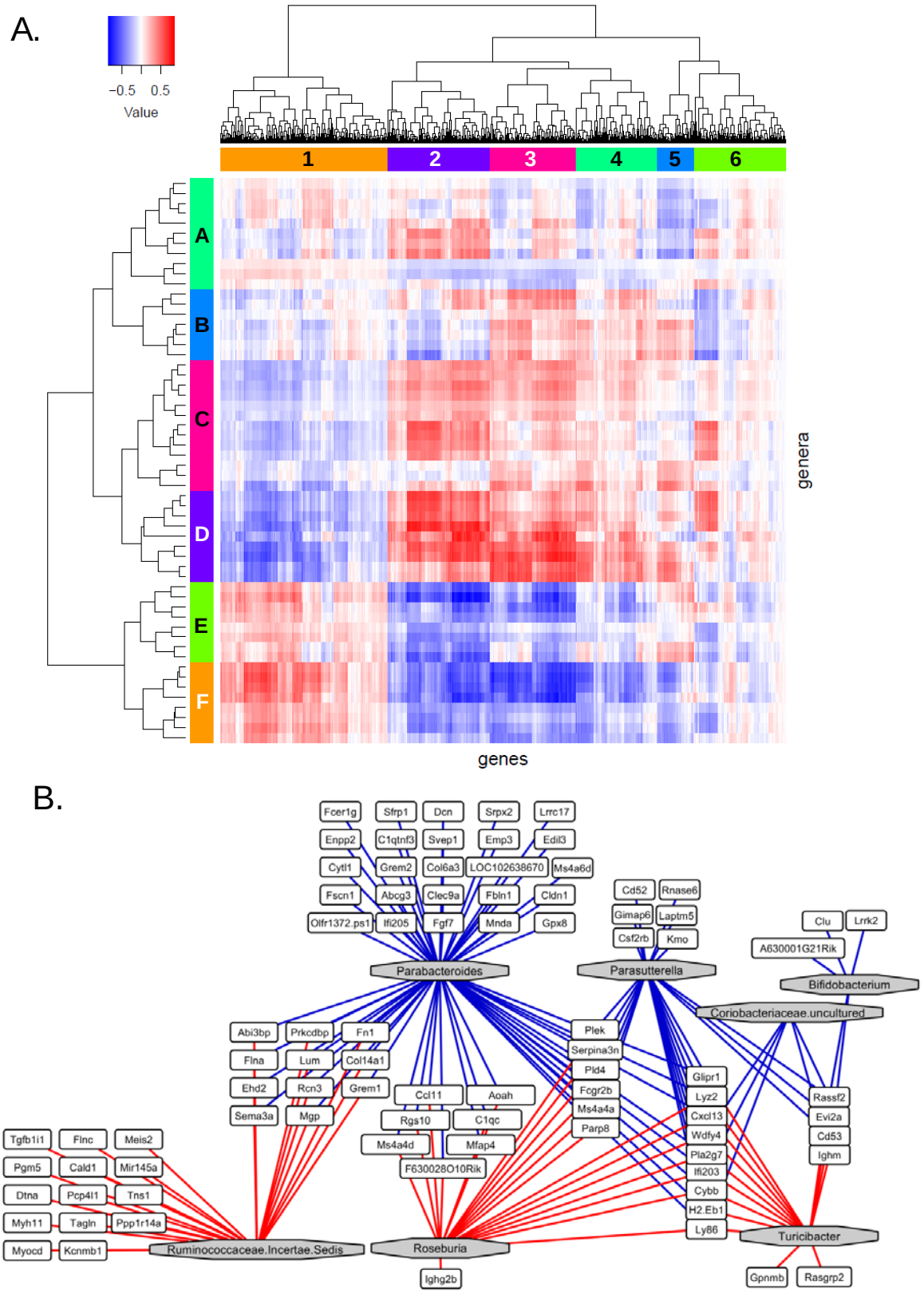

A.
−0.5
0.5
Value
1
2
3
4
5
6
A
B
C
D
E
F
genera
genes
B.
Fcer1g
Sfrp1
Dcn
Srpx2
Lrrc17
Enpp2
C1qtnf3
Svep1
Emp3
Edil3
Cytl1
Grem2
Col6a3
LOC102638670
Ms4a6d
Fscn1
Abcg3
Clec9a
Fbln1
Cldn1
Olfr1372.ps1
Ifi205
Fgf7
Mnda
Gpx8
Cd52
Rnase6
Gimap6
Laptm5
Csf2rb
Kmo
Clu
Lrrk2
A630001G21Rik
Parabacteroides
Parasutterella
Bifidobacterium
Coriobacteriaceae.uncultured
Abi3bp
Prkcdbp
Fn1
Flna
Lum
Col14a1
Ehd2
Rcn3
Grem1
Sema3a
Mgp
Ccl11
Aoah
Rgs10
C1qc
Ms4a4d
Mfap4
F630028O10Rik
Plek
Serpina3n
Pld4
Fcgr2b
Ms4a4a
Parp8
Glipr1
Lyz2
Cxcl13
Wdfy4
Pla2g7
Ifi203
Cybb
H2.Eb1
Ly86
Rassf2
Evi2a
Cd53
Ighm
Tgfb1i1
Flnc
Meis2
Pgm5
Cald1
Mir145a
Dtna
Pcp4l1
Tns1
Myh11
Tagln
Ppp1r14a
Myocd
Kcnmb1
Ruminococcaceae.Incertae.Sedis
Roseburia
Ighg2b
Turicibacter
Gpnmb
Rasgrp2

Figure 5

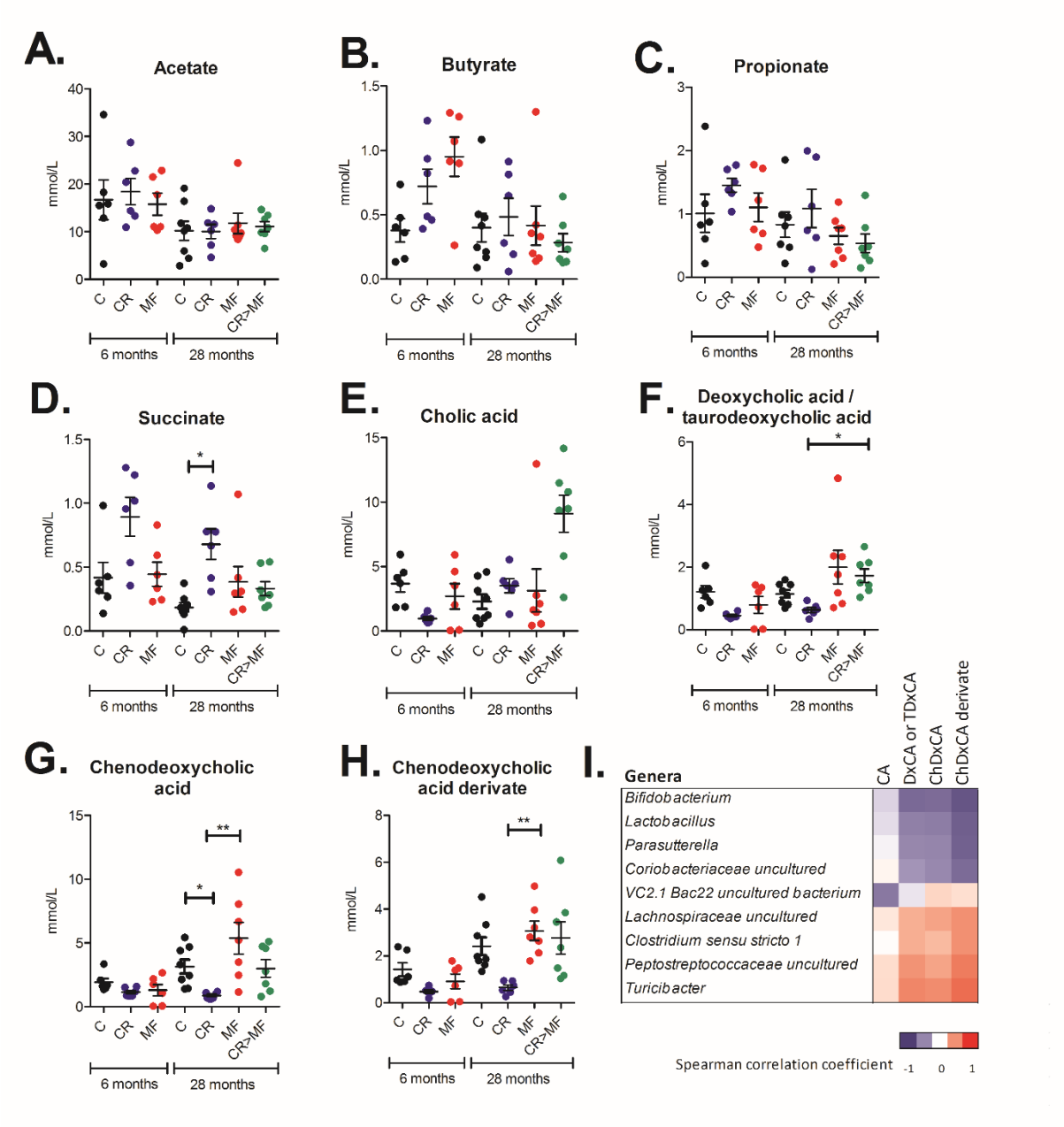

A.
Acetate
mmol/L
40
30
20
10
0
C CR MF C CR MF CR>MF
6 months
28 months
B.
Butyrate
mmol/L
1.5
1.0
0.5
0.0
C CR MF C CR MF CR>MF
6 months
28 months
C.
Propionate
mmol/L
3
2
1
0
C CR MF C CR MF CR>MF
6 months
28 months
D.
Succinate
mmol/L
1.5
1.0
0.5
0.0
*
C CR MF C CR MF CR>MF
6 months
28 months
E.
Cholic acid
mmol/L
15
10
5
0
C CR MF C CR MF CR>MF
6 months
28 months
F.
Deoxycholic acid / taurodeoxycholic acid
mmol/L
6
4
2
0
*
C CR MF C CR MF CR>MF
6 months
28 months
G.
Chenodeoxycholic acid
mmol/L
15
10
5
0
*
**
C CR MF C CR MF CR>MF
6 months
28 months
H.
Chenodeoxycholic acid derivate
mmol/L
8
6
4
2
0
**
C CR MF C CR MF CR>MF
6 months
28 months
I.
Genera
CA
DxCA or TDxCA
ChDxCA
ChDxCA derivate
Bifidobacterium
Lactobacillus
Parasutterella
Coriobacteriaceae uncultured
VC2.1 Bac22 uncultured bacterium
Lachnospiraceae uncultured
Clostridium sensu stricto 1
Peptostreptococcaceae uncultured
Turicibacter
Spearman correlation coefficient
-1
0
1

Figure 6

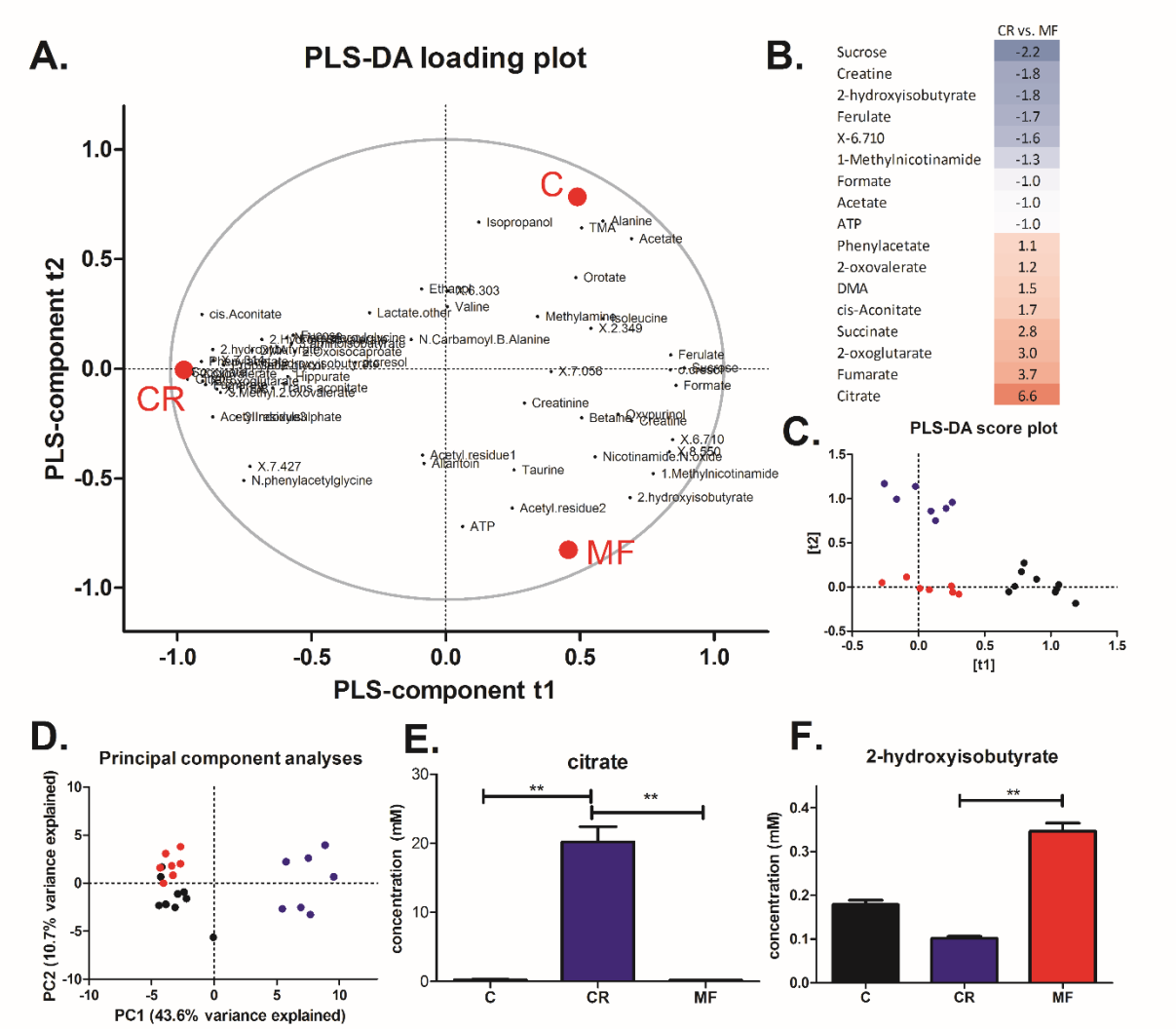
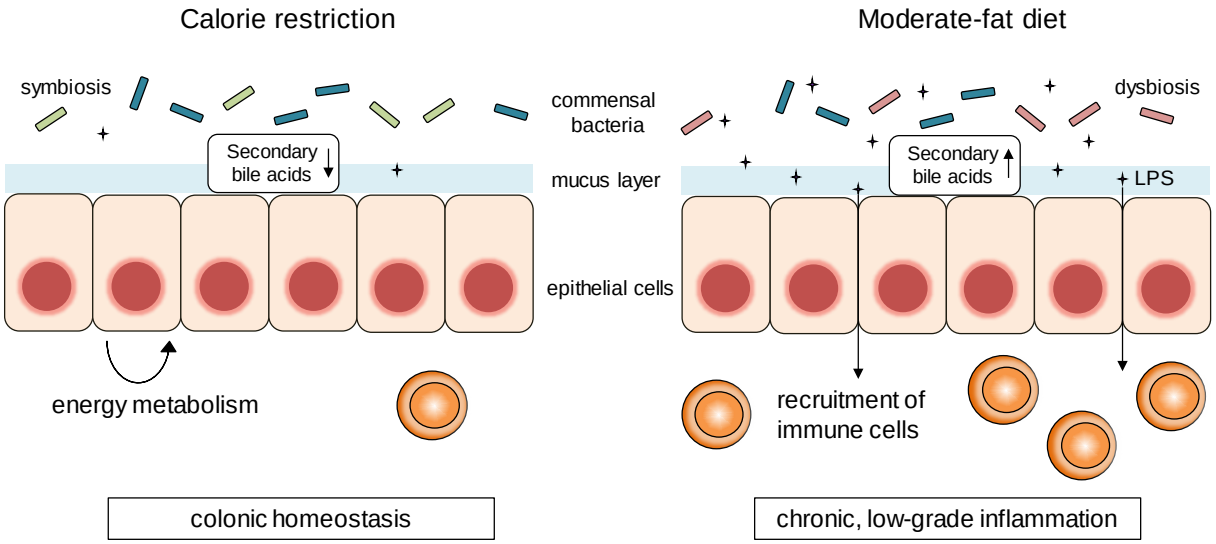

A.
PLS-DA loading plot
PLS-component t2
PLS-component t1
C
CR
MF
Isopropanol
TMA
Alanine
Acetate
Orotate
Ethanol
X.6.303
Valine
cis.Aconitate
Lactate.other
Methylamine
Isoleucine
X.2.349
N.Carbamoyl.B.Alanine
Ferulate
X.7.056
Sucrose
Formate
Creatinine
Betaine
Creatine
Oxypurinol
X.6.710
X.8.550
Nicotinamide.N.oxide
1.Methylnicotinamide
2.hydroxyisobutyrate
Acetyl.residue2
ATP
Acetyl.residue1
Allantoin
Taurine
X.7.427
N.phenylacetylglycine
B.
CR vs. MF
Sucrose -2.2
Creatine -1.8
2-hydroxyisobutyrate -1.8
Ferulate -1.7
X-6.710 -1.6
1-Methylnicotinamide -1.3
Formate -1.0
Acetate -1.0
ATP -1.0
Phenylacetate 1.1
2-oxovalerate 1.2
DMA 1.5
cis-Aconitate 1.7
Succinate 2.8
2-oxoglutarate 3.0
Fumarate 3.7
Citrate 6.6
C.
PLS-DA score plot
[t2]
[t1]
D.
Principal component analyses
PC2 (10.7% variance explained)
PC1 (43.6% variance explained)
E.
citrate
concentration (mM)
C
CR
MF
F.
2-hydroxyisobutyrate
concentration (mM)
C
CR
MF

Figure 7


Calorie restriction
Moderate-fat diet
symbiosis
commensal bacteria
dysbiosis
Secondary bile acids
mucus layer
Secondary bile acids
LPS
epithelial cells
energy metabolism
recruitment of immune cells
colonic homeostasis
chronic, low-grade inflammation